

149

A NUMERICAL INVESTIGATION OF
FILM COOLING AS AN ALTERNATE THERMAL
PROTECTION SYSTEM FOR SPACECRAFT DURING
ATMOSPHERIC REENTRY

A. M. Clausing

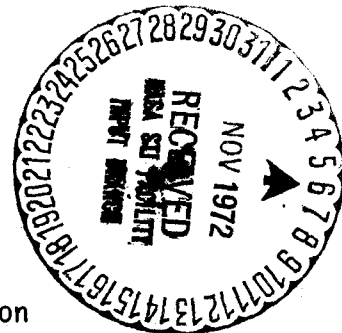
P. L. Kong

Heat Transfer Laboratory
Department of Mechanical and Industrial Engineering
Engineering Experiment Station
University of Illinois at Urbana-Champaign
Urbana, Illinois 61801

August 1972

ME TR 138-2

Research Sponsored by
National Aeronautics and Space Administration
under
Grant NGR 14-005-138
Final Report



(NASA-CR-112192) A NUMERICAL INVESTIGATION
OF FILM COOLING AS AN ALTERNATE THERMAL
PROTECTION SYSTEM FOR SPACECRAFT DURING
ATMOSPHERIC REENTRY A.M. Clausing, et al
(Illinois Univ.) Aug. 1972 63 p CSCI 20M G3/33
N73-10958 Unclas 16376

Reproduced by
NATIONAL TECHNICAL
INFORMATION SERVICE
U S Department of Commerce
Springfield VA 22151

A NUMERICAL INVESTIGATION OF
FILM COOLING AS AN ALTERNATE THERMAL
PROTECTION SYSTEM FOR SPACECRAFT DURING
ATMOSPHERIC REENTRY

A. M. Clausing

P. L. Kong

Heat Transfer Laboratory
Department of Mechanical and Industrial Engineering
Engineering Experiment Station
University of Illinois at Urbana-Champaign
Urbana, Illinois 61801

August 1972

ME TR 138-2

Research Sponsored by
National Aeronautics and Space Administration
under
Grant NGR 14-005-138
Final Report

	Page
ACKNOWLEDGMENTS	iv
NOMENCLATURE	v
LIST OF FIGURES	viii
1. INTRODUCTION	1
2. GENERAL ADVANCEMENTS IN FINITE DIFFERENCE METHODS APPLICABLE TO PARABOLIC PARTIAL DIFFERENTIAL EQUATIONS	3
2.1 Similarity and the Generalization of Finite- Difference Solutions	3
2.2 Practical Criteria for Choosing, <i>a priori</i> , the Increments in the Independent Variables	9
2.3 The Use of Nonuniform Grids in Finite-Difference Solutions--Numerical Integration with Constant Accuracy	13
3. FINITE DIFFERENCE ALGORITHMS WITH REPRESENTATIVE RESULTS	33
3.1 Algorithms for Compressible Flows of the Boundary Layer Type	33
3.2 A Turbulent Model and the Associated Finite Difference Procedure	38
4. RESULTS FROM THE STUDY OF FILM COOLING	45
5. REFERENCES	55

Preceding page blank

ACKNOWLEDGMENTS

The authors wish to express their sincere appreciation for the financial support of the National Aeronautics and Space Administration under Research Grant NGR 14-005-138. This study, which was of considerable educational value to both authors and which resulted in several advancements in finite-difference methods, would not have been possible without this financial support. Thanks are also due Mr. R. T. Swann, who suggested the problem, and Mr. G. Olsen, the contract monitor. They are members of the Thermal Protection Materials Branch of the Langley Research Center. The staff of the Mechanical Engineering Department Publications Office was also of considerable assistance throughout the project.

NOMENCLATURE

A_T	eddy viscosity
B_i	Biot modulus, hL/K
c_f'	local skin friction coefficient
E_T	truncation error
h	convective heat transfer coefficient
i	y-index, $y_i = (i - 1) \Delta y$ or $y_i = [(r_y^{i-1} - 1)/(r_y - 1)] \Delta y_1$
I	specific value of the index i
IS	$S = (IS - \frac{1}{2}) \Delta y$
k	thermal conductivity
ℓ	mixing length
L	thickness of infinite plate
M	$\left\{ \begin{array}{l} \frac{(\Delta y)^2 u_\infty}{v_\infty \Delta x}, \text{ boundary layer flow} \\ \frac{(\Delta y)^2}{\alpha \Delta t}, \text{ heat conduction} \end{array} \right.$
M_1	$\frac{(\Delta y_1)^2 u_\infty}{v_\infty \Delta x_1}$ or $\frac{(\Delta y_1)^2}{\alpha \Delta t_1}$
$M_{1, N}$	$\frac{(\Delta y_1)^2 u_\infty}{v_\infty \Delta x_N}$ or $\frac{(\Delta y_1)^2}{\alpha \Delta t_N}$
Ma	Mach number
n	x- or t-index, $x_n = n\Delta x$; or $x_n = [(r_x^n - 1)/(r_x - 1)] \Delta x_1$
N	specific value of the index n
p	index, $L = (p - 1) \Delta y$
Pr	Prandtl number
q	heat flow rate

q''	heat flux
r	common ratio in a geometric progression
Re	Reynolds number, $u_\infty x/\nu$
Re_1^\dagger	$u_\infty \Delta x_1/\nu$
S	slot height
t	time
T	temperature
u	x-component of velocity
\bar{u}	mean x-component of velocity, $u = \bar{u} + u'$
u'	component of turbulent velocity
$\overline{u'v'}$	mean of turbulent velocities
v	y-component of velocity
\bar{v}	mean y-component of velocity
v'	$v(\Delta x/\Delta y)$ or component of turbulent velocity
x, y	spatial coordinates
α	thermal diffusivity
γ	ratio of specific heats
δ	boundary layer thickness
δ_x, δ_x^2	central difference operators
∇	difference operator, defined in text
η	diffusion variable, $y/\sqrt{\alpha t}$ or $y\sqrt{u_\infty/\nu x}$
μ	dynamic viscosity
ν	kinematic viscosity
ρ	density
τ	shear stress
ω	exponent of property power law

Subscripts

0	initial condition
c	value before increment is changed
e	an equivalent or effective value
p	primary stream
s	temperature of surroundings or surface temperature; secondary stream
w	wall condition
∞	freestream condition

Superscripts

t	dimensionless quantity which contains an unspecified increment
*	dimensionless quantity
m	value obtained from the (m - 1)th increment-change
K	kth approximation obtained from the iterative application of the corrector

LIST OF FIGURES

	Page
Figure 2.1 The Influence of r_y on Accuracy--Heat Conduction in Semi-Infinite Solid	20
Figure 2.2 The Influence of r_y on Accuracy--The Blasius Problem	21
Figure 2.3 The Influence of r_t on Accuracy--Heat Conduction in Semi-Infinite Solid	22
Figure 2.4 The Influence of r_x on Accuracy--The Blasius Problem	23
Figure 2.5 The Influence of Increment Changes on Accuracy, $\Delta\eta_c = 0.15$ (Semi-Infinite Solid with Step Change in Surface Temperature)	30
Figure 2.6 The Influence of Increment Changes on Accuracy, $\Delta\eta_c = 0.10$ (Semi-Infinite Solid with Step Change in Surface Temperature)	31
Figure 2.7 The Influence of Increment Change on Accuracy, $\Delta\eta_c = 0.15$ (The Blasius Problem)	32
Figure 3.1 The Influence of r_x , r_y and Re_1^\dagger on the Accuracy of c_f' --Incompressible Turbulent Boundary Layer Flow	43
Figure 4.1 Nomenclature and Coordinate System for Flow Con- figuration being Studied	46
Figure 4.2 The Variation of the Temperature Distribution with N or ξ -- $\xi = 0.001107 N$	49
Figure 4.3 The Influence of T_s/T_p on the Normalized Heat Flux	50
Figure 4.4 The Influence of T_s/T_p on the Normalized Wall Shear Stress, Heat Flux, and Total Heat Flow Rate	51
Figure 4.5 The Influence of Ma_p on the Normalized Wall Shear Stress, Heat Flux, and Total Heat Flow Rate	52

1. INTRODUCTION

The basic objective of the research project was to determine the mass required to protect a surface during atmospheric re-entry by injecting a cold gas tangentially along the surface. Such a thermal protection system is known as film or slot cooling and is of considerable utility in many areas. It involves the mixing of the high enthalpy external stream with the coolant in the vicinity of a solid wall which is the surface being protected. A boundary layer forms along the wall, and eventually interacts strongly with the external mixing zone.

A consideration of this problem revealed that the boundary layer equations could be employed to approximate the most important flow configurations which occur in film cooling. However, even with this simplification, the equations to be solved are complex, non-linear, coupled partial differential equations. Due to the relative weakness of classical methods of boundary layer analysis, finite-difference methods were chosen as the best approach to the formidable problem under consideration.

A literature search revealed that the use of finite-difference techniques for the solution of the boundary layer equations has become popular only recently. Discrepancies and inconsistencies are common among recent publications. Many of the proposed techniques required an initial condition in the normal component of the velocity, v . This requirement is inconsistent with the boundary layer approximations. Other methods employed transformations which, in many cases, restricted the range of applicability of the technique.

Instead of blindly adopting a proposed technique and trying to force it to our problem, a more systematic study was deemed to be not only desirable but necessary. Otherwise numerous dead ends would probably have been encountered, and if a 'number' were obtained, it could have contained catastrophic errors. Also, the 'number' would have been the only product of the extensive efforts and the large digital computational costs. Necessary simplifications and changes in interest which often occur, could have meant that even correct answers would have been of little value. Hence, a relatively basic study of the application of finite-difference methods was undertaken with the objective of developing an algorithm capable of obtaining accurate solutions to film cooling problems.

An earlier report, Reference 1, contains the details of the proposed finite-difference algorithms and how they differ from those given in the literature. Numerous solutions were presented and graphical and tabular data were provided to establish the accuracy of the procedures. Further extensions including applications to turbulent flows are contained in Section 3 of this report.

As a consequence of the systematic study which was undertaken, several significant advancements in the general theory of finite-difference methods were made. The main items are:

1. Procedures for generalizing finite-difference solutions of parabolic partial differential equations,
2. Criteria for choosing *a priori* suitable increments in the independent variables for effecting accurate solutions to such equations, and
3. Procedures for reducing the computational effort beyond that accomplished through Item 1 (reductions of several orders of magnitude are common).

This material is presented in Section 2. In general, the procedures and criteria are not limited to any specific algorithm or problem; therefore, they should be of value to most investigators engaged in finite-difference solutions of partial differential equations of the parabolic type.

Section 4 contains results from the study of film cooling problems. Numerous results for incompressible and compressible laminar film cooling have been obtained. The initial turbulent results which have been obtained are not presented in Section 4. It was felt that it might be misleading to present the meager preliminary results currently available without further refinement. The investigation has not been completed; several assumptions need to be examined more carefully. The study will be continued, however, because it represents the subject of Mr. P. L. Kong's Ph.D. dissertation which is still incomplete. Additional publications containing further details and extensions are also planned.

2. GENERAL ADVANCEMENTS IN FINITE DIFFERENCE METHODS APPLICABLE TO PARABOLIC PARTIAL DIFFERENTIAL EQUATIONS

2.1 Similarity and the Generalization of Finite-Difference Solutions

Reference [2]*, a publication by one of the authors, contains a detailed discussion of the subject of similarity and the generalization of finite difference solutions. This section is a synopsis of [2], and it provides the necessary equations for the analyses and discussions given in the latter portions of the report.

Certain sets of partial differential equations can be reduced to sets of ordinary differential equations by appropriate transformations of the independent and dependent variables. Such solutions are generally designated as "similarity solutions" and are called "similar" because the profiles can be made congruent if they are plotted in coordinates that are made dimensionless with reference to the appropriate scale factors.

The search for similarity transformations and techniques of solving the resulting ordinary differential equations has been extensive. Impetus to the search for similarity transformations has been provided mainly by the supposed mathematical simplifications. For example, Schlichting [4] states that the reduction of a system of partial differential equations to one involving ordinary differential equations "evidently constitutes a considerable mathematical simplification of the problem." However, the ordinary differential equations that result are usually non-linear and effecting their solutions is difficult.

It was shown in [2] that the simplifications and advantages of similar problems are generally not lost if the solution to the original set of partial differential equations is effected with finite-difference methods in the *physical plane*. Furthermore, the similarity transformations can often be deduced by examining the governing difference equations written in terms of a generalized difference operator. If this property exists and is recognized, a large savings in computational effort is usually realized.

Since few practical problems are similar, the most significant

*Numbers in brackets refer to entries in Section 5, REFERENCES.

findings was that considerable savings can also be effected in non-similar problems. Not just one solution, but a whole family of solutions can often be effected with a single integration in the physical plane. One of the key steps in the generalization is to set up the problem such that the numerical calculation can be made without specifying the increments in the independent variables. Although the solution is effected in the physical plane, new dependent variables must sometimes be introduced in order to accomplish this objective. For example, the quantity v' , defined as $v\Delta x/\Delta y$, might be used in the numerical integration in place of the dependent variable v . Such quantities lead to the generalized dependent variables (the so-called similarity variables in similar problems) later in the analysis when the unspecified increments, Δx and Δy , are eliminated.

A parameter M that specifies the ratio between the spatial increment squared h^2 and the time increment Δt arises in all finite-difference algorithms of parabolic equations because of the nature of such equations. The definition of the particular parameter used in the analysis is dependent on the problem because other constants are introduced in order to reduce the parameter to a dimensionless quantity. The parameter is, of course, unique to the numerical solution. A key in the present analysis is the fact that the solution obtained with a stable and consistent finite-difference approximation in the limit as h and Δt approach zero is independent of $h^2/\Delta t$; that is, $h^2/\Delta t$ influences the results obtained with such finite-difference approximations, with finite values of h and Δt , only because this quantity influences the error.

The procedure for effecting the generalization of finite-difference solutions can be summarized as follows:

1. Set up the problem without specifying the increments in the independent variables.
2. Calculate N steps where N can be chosen arbitrarily.
3. Eliminate the increments from the dependent variables by introducing M , N , t (or the analogous spatial variable) and possibly other parameters.
4. For heuristic purposes, separate the solution into two parts; the exact solution which is independent of M , and the truncation error which is dependent on M .

5. Relate the indexes i , N and possibly others to the independent variables.
6. Reduce the number of variables by utilizing the fact that only the truncation error is dependent on M .

The mechanics become much clearer if one examines an actual problem. One of the simplest parabolic equations will be considered next; results from many additional examples are given in [2] and [3]. An infinite plate, which is initially isothermal and which suddenly begins to exchange heat by convection at one boundary, is the problem of interest. This is a nonsimilar problem, and one of the limiting cases of this problem, which will also be considered, is similar. The governing equation is

$$\frac{1}{\alpha} \frac{\partial T}{\partial t} = \frac{\partial^2 T}{\partial y^2} \quad (1)$$

where the constant α is the thermal diffusivity and T is the temperature. The initial and boundary conditions are

$$\left. \begin{aligned} T &= T_0 \text{ at } t = 0, & 0 \leq y \leq L \\ -k \frac{\partial T}{\partial y} \Big|_{y=0} &= h(T_s - T), & t > 0 \\ \frac{\partial T}{\partial y} \Big|_{y=L} &= 0, & t > 0 \end{aligned} \right\} \quad (2)$$

In replacing the derivatives in Eqs. (1) and (2) by difference quotients, the difference equations will be written in terms of a difference operator ∇ . ∇ represents any conceivable operator and is introduced in order to consider simultaneously all possible finite-difference representations of Eq. (3). The operator is not unique. If the discrete variables are defined as

$$\begin{aligned} t_n &= n(\Delta t) \\ y_i &= (i - 1)\Delta y \\ T_{i,n} &= T \text{ at } y_i \text{ and } t_n \end{aligned}$$

the finite-difference representation of Eq. (1) becomes

$$\frac{1}{\alpha} \frac{\nabla_t T_{i,n}^*}{\Delta t} = \frac{\nabla_y^2 T_{i,n}^*}{(\Delta y)^2}$$

or

$$\nabla_t T_{i,n}^* = \frac{1}{M} \nabla_y^2 T_{i,n}^* \quad (3)$$

where

$$M \equiv \frac{(\Delta y)^2}{\alpha \Delta t} \quad \text{and} \quad T^* \equiv \frac{T - T_o}{T_s - T_o}$$

The initial and boundary conditions in discrete form are

$$\left. \begin{aligned} T_{i,0}^* &= 0 \\ \nabla_y T_{1,n}^* &= \frac{h\Delta y}{k} (T_{1,n}^* - 1) = Bi^\dagger (T_{1,n}^* - 1) \\ \nabla_y T_{p,n}^* &= 0 \end{aligned} \right\} \quad (4)$$

where $L = (p - 1)\Delta y$ and $Bi^\dagger = h\Delta y/k$. Equations (3) and (4) reveal that

$$T_{i,n}^* = f_1(i,n,M,p,Bi^\dagger) \quad (5)$$

Equation (5) shows that the solution can be effected without specifying either Δy or Δt although quantities such as p , M , and Bi must be chosen before the numerical solution can be effected. Leaving Δy and Δt unspecified is, of course, unnecessary but it is a distinct advantage in some problems and is the key to eliminating redundant calculations. Equation (5) represents the results from Step 1 of the numbered procedure.

If one proceeds N -time steps (see Step 2), one obtains

$$T_{i,N}^* = f_1(i,N,M,p,Bi^\dagger)$$

Since this problem is relatively simple, the dependent variable does not contain any unspecified increments; hence, Step 3 is unnecessary. Otherwise it would lead to the relevant dependent variables.

Next, the solution is separated into two parts: the exact solution which is independent of M , and the truncation error, E_T , which is dependent on M (see Step 4).

$$T_{i,N}^* = f_2(i, N, p, Bi^\dagger) + E_T(i, N, M, p, Bi^\dagger) \quad (6)$$

The numerical integration yields f_1 ; f_2 is introduced for heuristic purposes. It is assumed throughout Section 2 that gross and round-off errors are negligible.

Since Δy and Δt are unspecified, the meaning of $T_{i,N}^*$ in the y - t plane remains to be determined (see Step 5). The relationship between the index i and the independent variables y_i and t_N follows from the definition of $y_i = (i - 1)\Delta y$ if M and t_N/N are introduced to eliminate Δy and Δt , respectively. The result is

$$y_i = (i - 1) \sqrt{\frac{M}{N}} \sqrt{\alpha t}$$

or

$$\eta_{i,N} \equiv \frac{y_i}{\sqrt{\alpha t_N}} = (i - 1) \sqrt{\frac{M}{N}} \quad (7)$$

Likewise,

$$\eta_{p,N} \equiv \frac{L}{\sqrt{\alpha t_N}} = (p - 1) \sqrt{\frac{M}{N}} \quad (8)$$

If Δy is eliminated from Bi^\dagger by introducing p , the Biot modulus follows

$$Bi \equiv \frac{hL}{k} = Bi^\dagger (p - 1) \quad (9)$$

Alternatively, Δy could have been eliminated by introducing $\sqrt{M/N} \sqrt{\alpha t_N}$

$$Bi' \equiv \frac{h \sqrt{\alpha t}}{k} = Bi^\dagger \sqrt{\frac{N}{M}} \quad (10)$$

If $\eta_{i,N}$, $\eta_{p,N}$ and Bi are introduced as new variables in place of N , p and Bi^\dagger , respectively, Eq. (6) becomes:

$$T_{i,N}^* = f_3(i, \eta_{i,N}, \eta_{p,N}, Bi) + E_T \quad (11)$$

Since f_3 is independent of M , M can be chosen for heuristic purposes to be proportional to N . Equations (7) and (8) shows that $\eta_{i,N}$ and $\eta_{p,N}$ are independent of N for this case; hence, Eq. (11) becomes (see Step 6)

$$T_i^* = f_4(\eta_i, \eta_p, Bi) + E_T \quad (12)$$

Alternatively, one could have used Bi' and obtained

$$T_i^* = f_4(\eta_i, \eta_p, Bi') + E_T \quad (13)$$

Because N and t_N are free to take on any value, the subscript N is deleted from $T_{i,N}^*$, t_N , $\eta_{i,N}$ and $\eta_{p,N}$. It is to be noted that the new independent variable, $\eta(\equiv y/\sqrt{\alpha t})$, arose from the governing equation, and it would have arisen regardless of the geometry, the initial condition, or the boundary conditions. This variable will be called the *diffusion variable* and is a meaningful dimensionless coordinate which governs the diffusion process. It is identical to the similarity variable in similar problems; however, its use and significance is by no means limited to similar problems. Equation (12) does not represent a unique result. A general discussion of alternative procedures is given in [2].

The boundary conditions and the finite length of the region L resulted in the parameters η_p and Bi . If L is large relative to $\sqrt{\alpha t}$, physical considerations show that the solution becomes independent of η_p , and one obtains from Eq. (13)

$$T_i^* = f(\eta_i, Bi') + E_T \quad (14)$$

Thus it is immediately clear that the whole family of solutions for this limiting case can be obtained with a single numerical integration in the physical plane. If h is large relative to $k/\sqrt{\alpha t}$, the solution becomes independent of Bi' ; that is, for a semi-infinite solid with a step change in surface temperature, the solution is

$$T_i^* = f(\eta_i) + E_T \quad (15)$$

This limiting solution is obviously a similar solution. If the finite size of the region is of importance but Bi is large, Eq. (8) becomes

$$T_i^* = f(\eta_i, \eta_p) + E_T \quad (16)$$

In the boundary layer examples given in [2], the diffusion variable, η , which resulted had an identical definition in the discrete plane

$$\eta_i = (i - 1)\sqrt{\frac{M}{N}}$$

η and M are of course different, they are:

$$\eta \equiv y \sqrt{\frac{u_\infty}{\nu x}} \quad \text{and} \quad M \equiv \frac{u_\infty (\Delta y)^2}{\nu \Delta x}$$

The definition of u_∞ was dependent on the particular problem.

The conclusions given in [2] are:

1. Similarity variables, if such quantities exist, can frequently be deduced from an analysis of the discrete form of the original differential equations and the respective boundary and initial conditions.
2. The generalization of the governing finite-difference equations can save considerable computational effort through the elimination of redundant calculations. The proposed analysis is applicable to both similar and non-similar problems.
3. Many similar solutions can be effected easily by solving the original partial differential equations in the physical plane by finite-difference methods. If numerical procedures are to be employed in effecting the solution, the supposed mathematical simplification introduced with the application of similarity transformations must be seriously questioned.

2.2 Practical Criteria for Choosing, *a priori*, the Increments in the Independent Variables

A major deficiency of numerical techniques is the inability to choose increments in the independent variables which will yield a reliable result. Young [5], in his survey of numerical analysis of elliptic and parabolic partial-differential equations, simply stated: "None of the papers which have been written on error estimation [35, 47-49, 51, 52, 65] can be said to come close to satisfying the needs of the practical computer user." A new criterion was proposed in [3] which partially alleviated this problem and many numerical results were presented in order to establish the validity of the proposed criterion.

The criterion essentially provides a practical means of taking into account the magnitudes of the derivations in choosing the increments

in the independent variables. A summary of the basis for the criterion follows and provides a starting point for the extensions given in Section 2.3. The reader is referred to [3] for additional information.

Consider the diffusion of heat, mass, or momentum into an infinite or semi-infinite medium. If the diffusion layer is thick, the spatial derivatives obviously are small. In addition, the mechanism of the diffusion process causes the time* derivatives to be small whenever the spatial derivatives are small. Hence, large spatial and time increments will give completely satisfactory results if the solution is desired at relatively large times. On the other hand, if the diffusion layer is thin, the spatial and time derivatives are large and the spatial increments in the region of influence and the time increments might have to be several orders of magnitude smaller in order to effect a meaningful solution. The key to a practical error criterion is that the approximate magnitude of the derivatives can be deduced from the thickness of the diffusion layer. The fact that the thickness of the diffusion layer is unknown is surmounted by relating it to a thickness in terms of a new dimensionless independent variable, the diffusion variable. Although the dimensional thickness of the diffusion layer may vary drastically with respect to time or the independent variable analogous to time, the thickness of the diffusion layer in terms of the diffusion variable, η , is a constant for a similar problem and usually varies over a relatively small range in non-similar problems. In addition, the diffusion thickness does not vary drastically from problem to problem. The diffusion thickness (see [3] for a precise definition) only varied between 1.4 and 5 for the diverse examples considered in Table 1 of [3] which included heat conduction problems, natural-convection boundary layer flows, and incompressible and compressible hydrodynamic boundary layers on flat plates and wedges. A notable exception is thermal boundary layers in liquid metals.

The hypothesis on which the error criterion is based is: The accuracy of a numerical solution can be estimated from the magnitude of the increment in the diffusion variable $\Delta\eta$, and this parameter provides a

*Throughout the discussion, one of the independent variables is assumed to be time. This is not always the case; e.g., consider two-dimensional steady-state boundary-layer problems.

means of intelligently choosing spatial and time increments for efficiently effecting finite-difference solutions of parabolic partial-differential equations in the physical plane. The number of grid points in the diffusion layer is the diffusion thickness divided by $\Delta\eta$; hence, a limit on the maximum value of $\Delta\eta$ fixes the minimum number of grid points which lie in the diffusion layer. It should be stressed that the solution is effected in the physical plane. The diffusion variable and the corresponding diffusion thickness are introduced in order to establish an error criterion.

The implications of a restriction on the magnitude of $\Delta\eta$ only become meaningful after a relationship is established between this quantity and the parameters of the discrete, physical plane. The procedure for determining this relationship was given in Section 2.1. Although the cases presented in [3] covered a wide range of physical problems, the relationship between the numerical parameters and the diffusion variable η was identical in all cases and is

$$\eta_i = (i - 1)\sqrt{\frac{M}{N}}$$

Hence, a criterion which restricts the magnitude of $\Delta\eta$, and in this manner guarantees several grid points within the diffusion layer, restricts the magnitude of $\sqrt{M/N}$. The proposed criterion is

$$\Delta\eta = \sqrt{\frac{M}{N}} < 0.3 \quad (16)$$

Criterion (16) guarantees between 5 and 18 grid points in the diffusion layer at the location of interest, $N(\Delta t)$ or $N(\Delta x)$, for the set of problems given in Table 1 of [3]. The criterion is designed to limit the truncation error and is not applicable if other errors are of importance. Round-off errors, programming errors, etc., can be accessed easily in many engineering problems by applying overall balances to the system, e.g., an energy balance, a force balance, or a mass balance.

Criterion (16) provides a practical means of choosing the increments in the independent variables for the numerical integration. It is simple to use and is applicable to a vast number of problems in a variety of fields. In the majority of cases investigated, the numerical

percent error lies between 0.2 and 2 percent at $\Delta\eta = 0.3$. The main exceptions were quantities which were asymptotically approaching zero; obviously, the percent error becomes meaningless in such cases.

If M/N were the only influences on the accuracy of the finite-difference solutions, the values of the increments should be chosen such that small values of M are obtained. For example, $M = 4$ and $N = 25$ would result in the same value of $\Delta\eta$ as $M = 40$ and $N = 250$, but the latter case would require an order of magnitude more computational effort.

Expressions for truncation errors would indicate that one should limit the increments in the independent variables Δy and Δt . In contrast, the present error hypothesis places limits on the sizes of $\Delta\eta$ and M . $\Delta\eta$ was introduced in order to take into account the magnitude of the derivatives; the minimum value of M must be restricted in order to avoid violations of physical laws. Criteria have been derived to avoid potential violations of physical laws for a variety of finite-difference methods [6,1]. These criteria are of the form

$$M \geq \zeta_1 \quad (17)$$

for heat-conduction problems, and

$$Mu_{i,N}^* \geq \zeta_2 \quad (18)$$

for boundary-layer problems. An additional criterion arises in boundary-layer problems if the energy equation is simultaneously being considered. The value of ζ is a function of the finite-difference method and the problem. It is of the order of one for problems with step changes in the neighborhood of the change. If physical laws are being violated, meaningless oscillations will occur. These can easily be detected from the results as long as they are monitored such that successive samples include both odd and even values of n . Hence, the form of the criterion and the order of magnitude of ζ is sufficient for the practical computer user. Criterion (18) shows that the numerical value of ζ_2 is of limited value anyway because $u_{i,n}^*$ is normally unknown; this is a characteristic of non-linear problems.

Numerous results were provided in [3] in order to establish the

utility of Criterion (16). These results will not be repeated here. The conclusions drawn in [3] from the numerous and varied test cases are:

1. The truncation error is strongly dependent on $\Delta\eta$ and relatively independent of most other parameters.
2. If M is sufficiently large to avoid violations of physical laws, it has a minor influence on the accuracy of finite-difference solutions effected with the Crank-Nicolson algorithm.
3. The criterion provides *a priori* means of choosing the increments in the independent variable which are required in order to effect a meaningful solution. The increments are directly related to the time or x -location of interest and to the relevant molecular diffusivity.
4. When the criterion was satisfied, engineering accuracy was obtained in all cases considered with the possible exception of compressible boundary layers at high Mach numbers. The reason for this exception was given.
5. The criterion gives satisfactory results for non-similar problems, for non-linear problems, and for diffusion in finite regions. It should be used with caution, however, in areas which are vastly different from the examples used in the present verifications. Although the form of the criterion should remain applicable, the constant 0.3 may prove to be too small or too large.

2.3 The Use of Nonuniform Grids in Finite-Difference Solutions--Numerical Integration with Constant Accuracy

The accuracy of a finite-difference solution to a diffusion problem usually increases as time* increases if the increments are held constant. Usually the derivatives are becoming smaller; hence, expressions for the local truncation error clearly show why the error decreases in such cases.

*Again, throughout the discussion in Section 2.3, one of the independent variables is assumed to be time. This is not always the case; e.g., x is the analogous independent variable in the boundary layer problems.

Small spatial and time increments are generally required in order to effect an accurate solution at small times, whereas large spatial and time increments give completely satisfactory results if large times are of interest.

The procedure given in Section 2.1, which enables one to leave the increments unspecified, greatly alleviates this difficulty in some cases by leaving the increments unspecified. Obviously, the results obtained after N steps can be applied at any time if the time increment has not been specified. Although the magnitude of the problem has been reduced by leaving the increments unspecified, not all difficulties and expensive calculations have been eliminated. One area which leads to costly calculations is nonsimilar problems if large ranges of the additional parameters are of interest. For example, consider the parameters η_p and Bi in Eqs. (12 and (14), respectively, of Section 2.1. Even though a whole family of solutions is obtained with a single integration, the calculation still can be expensive. A turbulent boundary layer flow presents difficulties because small increments are required in order to include grid points in the non-turbulent sublayer. However, the thickness of this layer is small relative to the thickness of the boundary layer. The use of a uniform network is clearly unacceptable in this case.

Furthermore, leaving the increments unspecified in no way removes the dependency of the accuracy on the number of time steps, N. Ideally, a procedure which results in a solution whose accuracy is independent of the number of time steps is desired.

The use of a nonuniform grid is by no means a new idea. Many investigators simply double or triple the time and/or spatial increments every so often. For example, Pletcher [7] used the following distribution in the y-increment in his finite-difference solution of a turbulent boundary layer.

$$\Delta y^+ = 4 \quad 0 < y^+ \leq 80$$

$$\Delta y^+ = 10 \quad 80 < y^+ \leq 180$$

$$\Delta y^+ = 20 \quad 180 < y^+ \leq 380$$

$$\Delta y^+ = 40 \quad 380 < y^+ \leq 1180$$

$$\Delta y^+ = 100 \quad 1180 < y^+$$

A procedure like Pletcher's suffers from two main disadvantages. First, the changes in the local truncation error are large and abrupt. Since the local truncation error due to the y-derivatives is of the order of $(\Delta y)^2$ in Pletcher's algorithm, a change by a factor of either 4 or 6.25 occurs from one region to the next. Second, the local truncation error at the interface between any two regions is, in general, larger than that in either region. Hence, some of the desired gain is offset by the large truncation error which occurs at these interfaces. Abrupt changes in the time increments usually suffer from only the first of these two disadvantages. This is because most numerical procedures employ forward difference quotients for the time derivatives.

Smith and Cebeci [8] appear to have been one of the first to use a more smoothly varying grid. They employed a geometrical progression for the variation of the increment in their transformed coordinate normal to the surface in a turbulent boundary layer study. Calling this coordinate y, successive y increments were

$$\Delta y_1, r\Delta y_1, r^2\Delta y_1, r^3\Delta y_1, \text{ etc.}$$

Hence,

$$\Delta y_i = r\Delta y_{i-1}, \quad i > 1 \quad (19)$$

or

$$\Delta y_i = r^{i-1}\Delta y_1, \quad i \geq 1 \quad (20)$$

where $r \geq 1$. It follows that

$$y_i = \Delta y_1 + r\Delta y_1 + r^2\Delta y_1 + \dots + r^{i-1}\Delta y_1$$

or

$$y_i = \Delta y_1 \left(\frac{r^{i-1} - 1}{r - 1} \right) \quad (21)$$

Smith and Cebeci did not discuss the influence of r on their accuracy, nor did they indicate any basis for choosing r or a geometrical progression other than the following: "This variable grid system permits shorter steps close to the wall and larger steps away from the wall, and thus maintains computing accuracy." They employed an *arbitrary* spacing in the other transformed coordinate. More recent studies by Harris [9] and Adams [10] also used a geometrical progression and

credited Smith and Cebeci for proposing it.

It is interesting to note that so far no one has been successful in providing a rational, systematic means of varying the grid spacing. A basis or criterion for establishing the manner in which the increments should be varied has not been found.

The objective is to vary the spatial and time increments during the integration such that the accuracy of the results is independent of both the time and the spatial location. Implicit in this objective is the requirement that the process remain stable and satisfy the fundamental laws governing the phenomenon, e.g., the second law of thermodynamics. It is probably impossible to fully accomplish this objective. However, the criterion recently developed by Clausing [3] appears to provide a means of approaching this subject in a rational manner. Heretofore, a basic ingredient, a practical error criterion, was missing.

It was established in [3] (also see Section 2.2) that the accuracy of finite-difference solutions is strongly dependent on the increment in the diffusion variable, $\Delta\eta$. The proposed criterion is:

$$\Delta\eta = \sqrt{\frac{M}{N}} < 0.3 \quad (16)$$

The relationship between the diffusion variable and the parameters of the discrete physical plane can be established with the procedures outlined in Sections 2.1 and 2.2. The stated objective when translated into Criterion (16) through Criterion (18) requires that the calculation proceed in a manner such that $\Delta\eta$ remains relatively constant. Simultaneously, one cannot allow M to become too small. Clearly, the y -increments must be dependent on both y and time. Also, the time increment cannot be chosen independently, but is strongly dependent on the variation of Δy_1 with time. Smith and Cebeci [8], Harris [9], and Adams [10] use increments in the transformed variable normal to the wall which were independent of the other coordinate. Furthermore, all three of these investigators used an "arbitrary" or constant spacing of the grid points in the other direction. The two increments were in no way related to each other.

Since large changes in Δy and Δt at arbitrary values of i and/or n are to be avoided if possible, geometrical progressions in both increments

will be considered. Geometrical progressions appear to be a natural choice for diffusion problems of the boundary layer type. Initially Δy will be assumed to be independent of time; the problem will be generalized further later in this section. Hence,

$$\Delta y_i \equiv r_y^{i-1} \Delta y_1, \quad i \geq 1 \quad (22)$$

and

$$\Delta t_n \equiv r_t^{n-1} \Delta t_1, \quad n \geq 1 \quad (23)$$

therefore,

$$y_i = \Delta y_1 \left(\frac{r_y^{i-1} - 1}{r_y - 1} \right), \quad i \geq 1 \quad (24)$$

and

$$t_n = \Delta t_1 \left(\frac{r_t^n - 1}{r_t - 1} \right), \quad n \geq 0 \quad (25)$$

If the "edge" of the diffusion layer lies at $i = I$ and the calculation is to proceed to $n = N$, the equivalent values required with a uniform grid with increments of Δy_1 and Δt_1 are, respectively,

$$I_e = 1 + \left(\frac{r_y^{I-1} - 1}{r_y - 1} \right) \quad (26)$$

and

$$N_e = \frac{(r_t^N - 1)}{(r_t - 1)} \quad (27)$$

The savings in computational effort which results from these geometrical progressions can be deduced from Table 2.1. This table shows the influence of r and N on N_e/N or r and $(I - 1)$ on $(I_e - 1)/(I - 1)$. Typically, one would probably use a value of I which is less than 100 and N which is less than 1,000; hence, the upper half of the table is designed for determining I_e and the lower half for determining N_e .

Two problems will be used to show the influences of r_y and r_t on the accuracy: heat flow in a semi-infinite solid with a step change in surface temperature and incompressible laminar boundary layer flow over

Table 2.1 The Influence of r on the Effective Values of I and N

r N or (I - 1)	N/N _e or (I _e - 1)/(I - 1)							
	1.001	1.002	1.005	1.010	1.020	1.050	1.100	1.200
5	1.0	1.0	1.0	1.0	1.0	1.1	1.2	1.5
10	1.0	1.0	1.0	1.0	1.1	1.3	1.6	2.6
15	1.0	1.0	1.0	1.1	1.1	1.4	2.1	4.8
20	1.0	1.0	1.0	1.1	1.2	1.6	2.9	9.3
25	1.0	1.0	1.1	1.1	1.3	1.9	3.9	18.9
30	1.0	1.0	1.1	1.2	1.4	2.2	5.5	39.4
35	1.0	1.0	1.1	1.2	1.4	2.6	7.7	84.2
40	1.0	1.0	1.1	1.2	1.5	3.0	11.1	183
45	1.0	1.0	1.1	1.3	1.6	3.6	16.0	406
50	1.0	1.1	1.1	1.3	1.7	4.2	23.3	910
55	1.0	1.1	1.1	1.3	1.8	5.0	34.2	2059
60	1.0	1.1	1.2	1.4	1.9	5.9	50.6	4696
70	1.0	1.1	1.2	1.4	2.1	8.4	112	24920
80	1.0	1.1	1.2	1.5	2.4	12.1	256	> 10 ⁵
100	1.0	1.1	1.3	1.7	3.1	26.1	1378	
150	1.1	1.2	1.5	2.3	6.2	200	> 10 ⁵	
200	1.1	1.2	1.7	3.2	12.9	1729		
250	1.1	1.3	2.0	4.4	28.1	15864		
300	1.2	1.4	2.3	6.3	63.2	> 10 ⁵		
350	1.2	1.4	2.7	9.0	146			
400	1.2	1.5	3.2	13.1	344			
500	1.3	1.7	4.4	28.8	1996			
600	1.4	1.9	6.3	65.1	12051			
700	1.4	2.2	9.1	151	74837			
800	1.5	2.5	13.3	358	> 10 ⁵			
900	1.6	2.8	19.6	861				
1000	1.7	3.2	29.1	2096				

a flat plate, the Blasius problem. (See examples 1 and 3 of [2] for governing equations and other details.) If one chooses $M = 10$ and were to integrate to $\Delta\eta = 0.05$, a uniform grid would require $I \approx 140$ and $N = 4,000$. A total of approximately one-half million grid points would result if a constant value of I is employed. This could be reduced by approximately one-third if I were varied as the thickness of the diffusion layer increased. Using $r_y = r_t = r_x = 1.05$ requires $I = 45$ and $N = 109$, a total of approximately 4,900 grid points with a rectangular grid. This represents a reduction in the computational effort of three orders of magnitude. Integrating an equivalent of 4,000 steps is not unrealistic. If $\Delta\eta$ must be less than 0.3 in order to obtain the desired accuracy, $N_e = 4,000$ would result in a useful solution over a time period from t_0 to $36 t_0$ or a Reynolds number ranging from Re_0 to $36 Re_0$. If $I = 150$ and $N = 4,000$ were actually used, round-off error would probably strongly influence the results.

The influence of r_y on the accuracy is shown in Figs. 2.1 and 2.2. Figure 2.1 shows the variation of the percent error in the heat flux through the surface with $\Delta\eta$ for the heat conduction problem. Six different values of r_y are used. Figure 2.2 gives results for the Blasius problem. Both sets of results were obtained with r_t (or r_x) equal to one. Figure 2.1 shows that, relative to the influence of $\Delta\eta$, the influence of r_y is small if r_y is less than 1.3. The apparent influence of r_y is greater for the Blasius problem but the original error curve is misleadingly small because it parallels the abscissa. The approximate number of grid points required in the y -direction at $\Delta\eta = 0.15$ for $r_y = 1, 1.05$, and 1.3 is 48, 26, and 11, respectively.

Figures 2.3 and 2.4 show the influence of r_t (or r_x) for these same two problems. A value of $r_y = 1.05$ was chosen in both cases because the integration was carried to rather small values of $\Delta\eta$. The integration to $\Delta\eta = 0.05$ required 1,600, 91, and 32 steps for r_t (or r_x) equal to 1.0, 1.05, and 1.2, respectively. The computational effort required to integrate to $\Delta\eta = 0.05$ with $r_y = 1.05$ and $r_t = 1.2$ was less than 1 percent of that required with a uniform grid. The influence of r_t or r_x on the accuracy is smaller than the influence of r_y , provided that the calculation

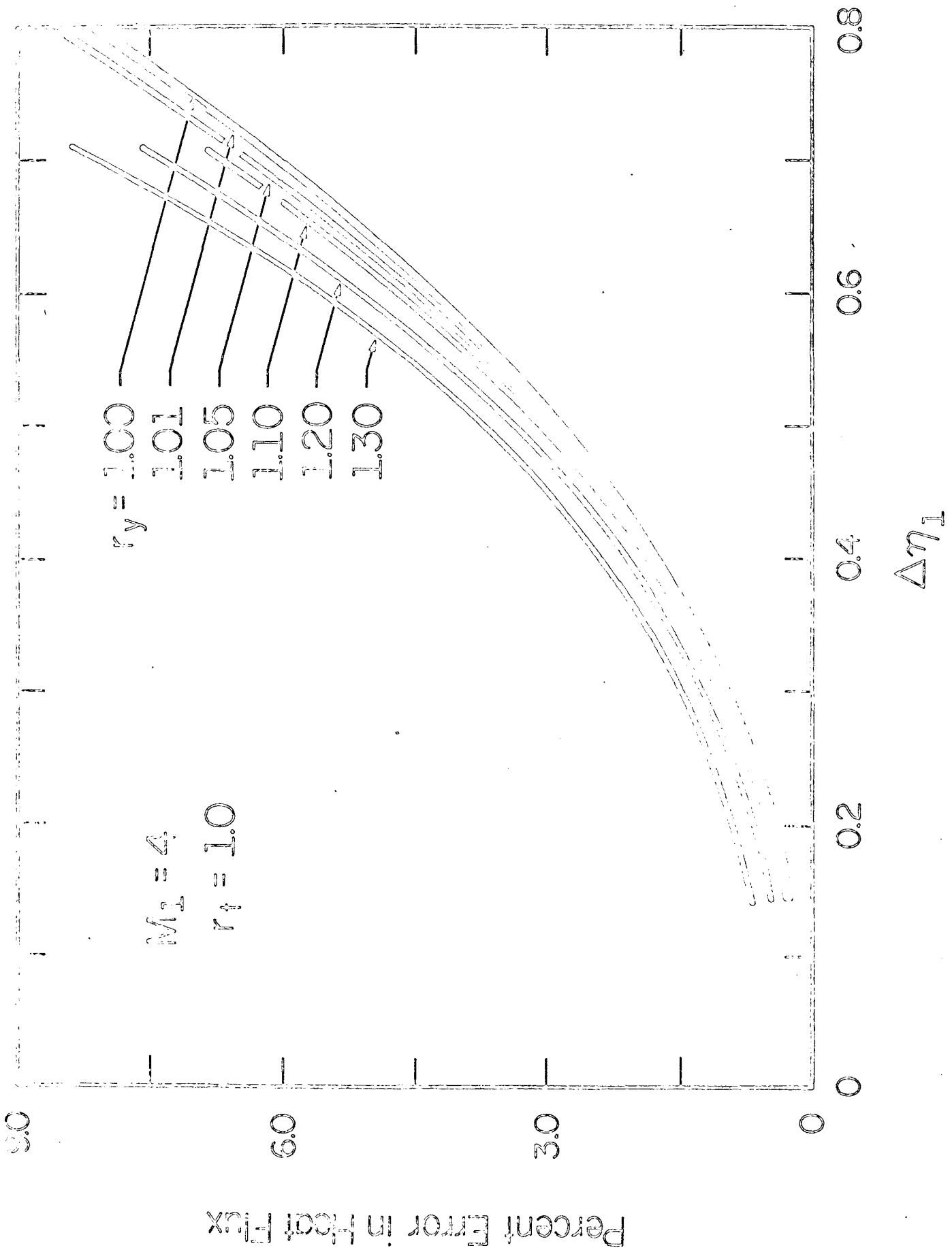


Figure 2.1 The Influence of r_y on Accuracy--Heat Conduction in Semi-Infinite Solid

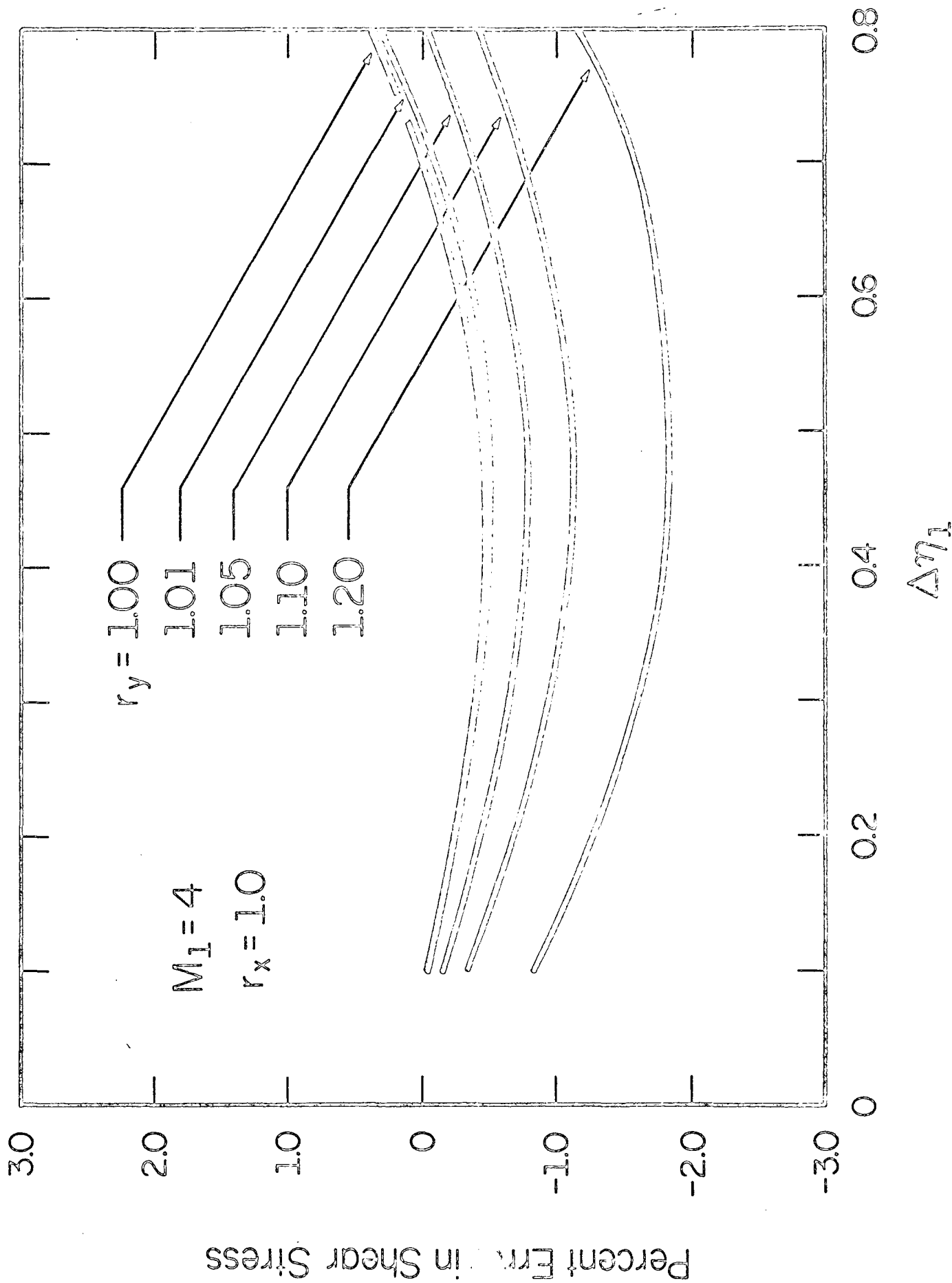


Figure 2.2 The Influence of r_y on Accuracy--The Blasius Problem

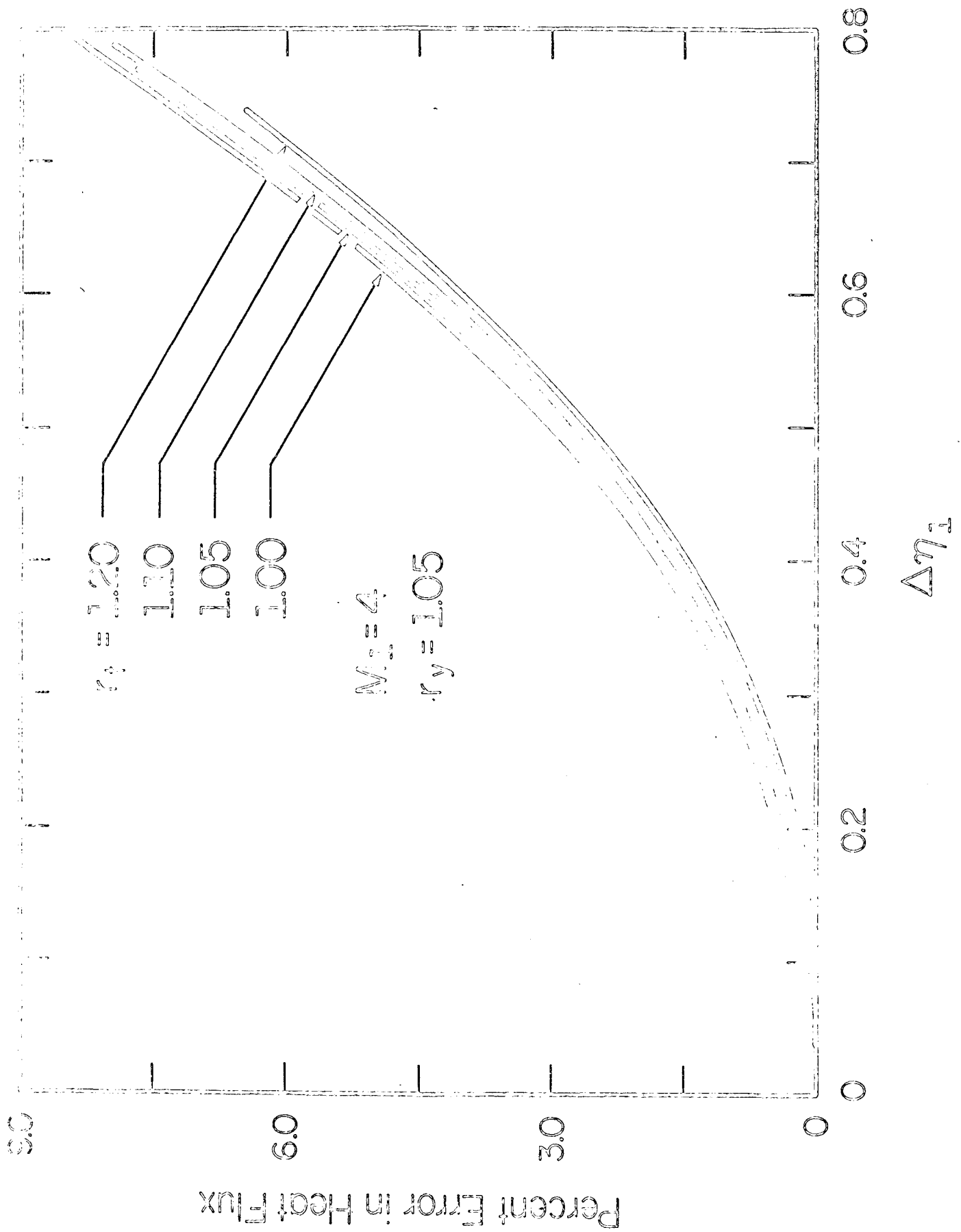


Figure 2.3 The Influence of r_1 on Accuracy--Heat Conduction in Semi-Infinite Solid

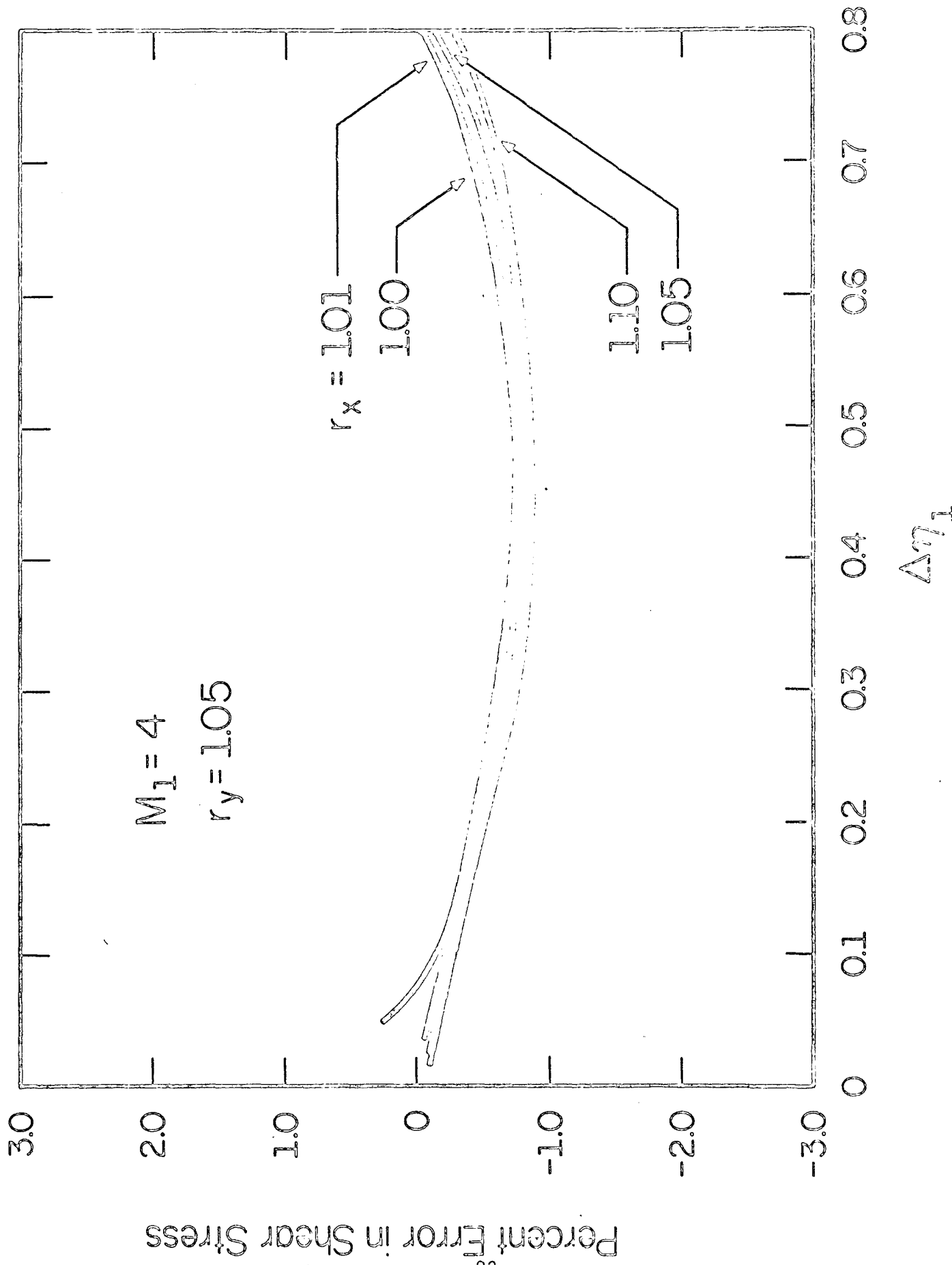


Figure 2.4 The Influence of r_x on Accuracy--The Blasius Problem

avoids violations of physical laws. The influence of r_t or r_x is essentially negligible compared to the influence of $\Delta\eta$ if r is less than approximately 1.1.

If a nonuniform grid is employed, expressions for η_i and $\Delta\eta$ must again be derived. The following definitions will be used:

$$M_1 \equiv \frac{(\Delta y_1)^2}{\alpha \Delta t_1} \quad (28)$$

$$M_{1, N} \equiv \frac{(\Delta y_1)^2}{\alpha \Delta t_N} \quad (29)$$

and

$$\Delta\eta_1 \equiv \eta_{2, N} - \eta_{1, N} \quad (30)$$

Since Δy_1 and Δt_1 are unspecified, the meaning of $T_{i, N}^*$ in the y - t plane remains to be determined. The procedure with a nonuniform grid is identical to that used with a uniform grid. One starts with the definition of y_i , Eq. (24) in this case. M_1 is introduced in order to eliminate Δy_1 . This introduces Δt_1 which is eliminated by introducing N and t_N , Eq. (25). This gives

$$\eta_{i, N} \equiv \frac{y_i}{\sqrt{\alpha t_N}} = \left(\frac{r_y^{i-1} - 1}{r_y - 1} \right) \left[\frac{M_1}{\frac{r_t^N - 1}{r_t - 1}} \right]^{\frac{1}{2}} \quad (31)$$

or if N_e is introduced

$$\eta_i = \frac{r_y^{i-1} - 1}{r_y - 1} \sqrt{\frac{M_1}{N_e}} \quad (32)$$

The definition of $\Delta\eta_1$, Eq. (30) combined with Eq. (32) gives:

$$\Delta\eta_1 = \sqrt{\frac{M_1}{N_e}} \quad (33)$$

The only differences between these results and the expressions obtained for a compressible or incompressible boundary layer on a flat

plate lie in the definitions of η and M_1 . Although $\Delta\eta_1$ is the smallest increment in this variable, it is the logical choice for use in the error criterion, Criterion (16). This is demonstrated by the error curves given in Figs. 2.1 through 2.4. $M_{1,N}$ is the smallest value of M and should be used in Criteria (17) and (18).

Equation (33) shows that $\Delta\eta$ is by no means constant. Indeed, smaller values of $\Delta\eta$ are generated much more quickly if $r_t > 1$. In addition, Eqs. (23) and (24) give

$$M_{1,N} = \frac{M_1}{r_t^{N-1}} \quad (34)$$

Hence, $M_{1,N}$ is growing smaller with increasing N . Clearly, if Δy_1 is independent of time, our objective cannot be accomplished. Dangerously small values of M will be generated and the calculation will become inefficient due to unnecessarily small values of Δy_i . This will, in turn, result in such large values of I that round-off error may become of importance.

An obvious choice for meeting the objective is to assume Δy is given by

$$\Delta y_{i,N} = r_{ty}^{N-1} r_y^{i-1} \Delta y_1 = r_y^{i-1} \Delta y_{1,N} \quad (35)$$

The corresponding expression for $\Delta\eta_1$ becomes

$$\Delta\eta_1 = r_{ty}^{N-1} \left[\frac{M_1}{\frac{r_t^N - 1}{r_t - 1}} \right]^{1/2} \quad (36)$$

Since

$$M_{1,N} = \frac{(\Delta y_{1,N})^2}{\alpha \Delta t_N} = \frac{\{r_{ty}^{N-1} \Delta y_1\}^2}{\alpha r_t^{N-1} \Delta t_1}$$

$M_{1,N}$ would become independent of N if one chose

$$r_{ty} = \sqrt{r_t} \quad (37)$$

If this value of r_{ty} is substituted into Eq. (36), $\Delta\eta_1$ becomes

$$\Delta\eta_1 = \left\{ \frac{r_t^{N-1} (r_t - 1) M_1}{r_t^N - 1} \right\}^{1/2} \quad (38)$$

Equation (38) shows that $\Delta\eta_1$ would be strongly dependent on N only if N were small. The asymptotic value of $\Delta\eta_1$ follows from Eq. (38) and is

$$\lim_{N \rightarrow \infty} \Delta\eta_1 = \left[\frac{r_t - 1}{r_t} M_1 \right]^{1/2} \quad (39)$$

Thus, the asymptotic value of $\Delta\eta_1$ has been changed from zero to a finite constant by introducing r_{ty} and relating it to r_t such that M is a constant. M_1 and r_t can be chosen in order to give the desired asymptotic value of $\Delta\eta_1$, i.e., the desired accuracy.

Although both objectives would appear to have been accomplished (at least to some degree) by this procedure, the use of r_{ty} causes a serious problem. A nonorthogonal set of grid lines results. The grid is orthogonal only at $i = 1$ and becomes more and more skewed with increasing i . If this skewness is ignored, serious error can result in some problems. To correctly take the skewness into account would be extremely difficult or impossible for complex sets of equations. Thus, the use of r_{yt} appears to be impractical.

Since any continuous variation of Δy_1 with N would result in a skewed network, a periodic abrupt change appears necessary in order to approach the main objective. The proposed procedure is to periodically drop every other grid point in the y -direction such that the value of $\Delta\eta_1$ will not become less than some prescribed value, $\Delta\eta_c$. When every other grid point is dropped, $\Delta\eta$ will approximately double; hence, the accuracy will not be constant but it will only vary over a narrow range. Criterion (16) suggests $\Delta\eta_c$ should be approximately 0.1 or 0.15.

If the superscript m is introduced to identify the successive values of Δy_1 , and $\Delta y_1^1 \equiv \Delta y_1$, then:

$$\Delta y_1^m = (1 + r_y^{m-1}) \Delta y_1^{m-1}, \quad m > 1 \quad (40)$$

Deleting every other grid point results in another geometric progression but with a different value of r_y . Successive values of r_y^m are

$$r_y^m = (r_y^{m-1})^2, m > 1 \quad (41)$$

r_y^1 must be chosen with this progression in mind. In general, the calculation should probably be limited to three or four changes. Equation (40) shows that M will change by a factor of $(1 + r_y^{m-1})^2$ when the y -increment is changed. An expression for determining r_t such that M remains within reasonable bounds can be derived by relating the value of N, N_c , at which this change occurs to the value of N which gives the desired value of $M_{1,N}$. Equation (33) is

$$\Delta\eta_c = \left[\frac{M_1 (r_t - 1)}{r_t^{N_c} - 1} \right]^{1/2}$$

Also assume

$$\frac{M_1}{M_{1,N}} = C = r_t^{N_c - 1} \quad (42)$$

where C is a constant. The most logical choice for this constant is probably 4. Since $r_t^{N_c} \approx r_t^{N_c - 1}$, Eqs. (33) and (42) give:

$$r_t \approx \frac{(\Delta\eta_c)^2 (C - 1)}{M_1} + 1 \quad (43)$$

If this value of r_t is used, $M_{1,N}$ will vary between M_1 and M_1/C for $m = 1$. The asymptotic, minimum $M_{1,N}$ can easily be shown to be

$$\lim_{m \rightarrow \infty} M_{1,N} = \frac{M_1}{C - 1} \quad (44)$$

Due to the variation of r_y with m , I is growing progressively smaller. A slight modification which definitely warrants study would be to keep I fixed. Every other grid point would then be deleted based on η_1 , instead of $\Delta\eta_1$. Initially, the two procedures would give identical results; however, as m increases significant differences in the various parameters would arise. Smaller values of $\Delta\eta_1^m$ would result in order to keep I constant as r_y becomes progressively larger.

The progression of r_y and I for two different values of $\Delta\eta_c$ are given in Table 2.2. The error curves which were obtained with the parameters given in Table 2.2 for the problem of a semi-infinite solid with a step change in surface temperature are given in Figs. 2.5 and 2.6. Since the error curves for these cases lie so close together even with the greatly expanded scale used, the spread of the seven additional curves between $\Delta\eta_c$ and approximately $2\Delta\eta_c$ are simply indicated by a cross-hatched area. The error was always less than 0.9 percent and greater than 0.2 percent with $\Delta\eta_c$ equal to 0.15 and for N between 16 and 289. The maximum and minimum errors were reduced to 0.4 percent and 0.1 percent with $\Delta\eta_c = 0.10$ and N between 37 and 369. M varied between 2.0 and 0.5 for the first error curve ($m = 1$), and it varied between 2.8 and 0.67 (see Eq. (44)) for the last error curve, $m = 7$. The corresponding range of N_e for the two cases is approximately from 21 to 4×10^5 and 48 to 9×10^5 . A uniform grid with the initial spatial and time increments would have required approximately 200,000 times more computational effort!

Figure 2.7 shows a set of error curves for the Blasius problem. The parameters used are the same as those employed in Case I of the conduction problem and Table 2.2 is applicable. It is noted that the larger values of r_y have a much smaller influence on the accuracy if the calculation is begun with small values of r_y . For example, compare the results of Figs. 2.1 and 2.2 with Figs. 2.5 through 2.7.

The tremendous savings in computational effort makes the general procedure look indeed attractive. Much further study is required and general conclusions cannot be drawn at this time. It is clear that the possible savings in computational effort in the solution of turbulent boundary layer problems and other nonsimilar problems is not merely a factor of 2 or 3 but several orders of magnitude.

Table 2.2 Parameters Corresponding to Figs. 2.5 and 2.6 Showing Influences of Increment Changes

Case I Case II

Chosen: r_y 1.0025 1.0025

$\Delta\eta_c$ 0.15 0.10

I_e 48 71

$\eta_I = \Delta\eta_c (I_e - 1)$ 7.0 7.0

M_1 2.0 2.0

Results of Calculations:

r_t (Eq. 43) 1.03375 1.0150

	m	1	2	3	4	5	6	7
	r_y	1.0025	1.005	1.010	1.020	1.041	1.083	1.173
Case I	I	45	43	40	34	28	21	15
	N_c	42	78	118	160	202	249	289
Case II	I	66	54	45	35	25	17	11
	N_c	94	173	262	355	449	545	644

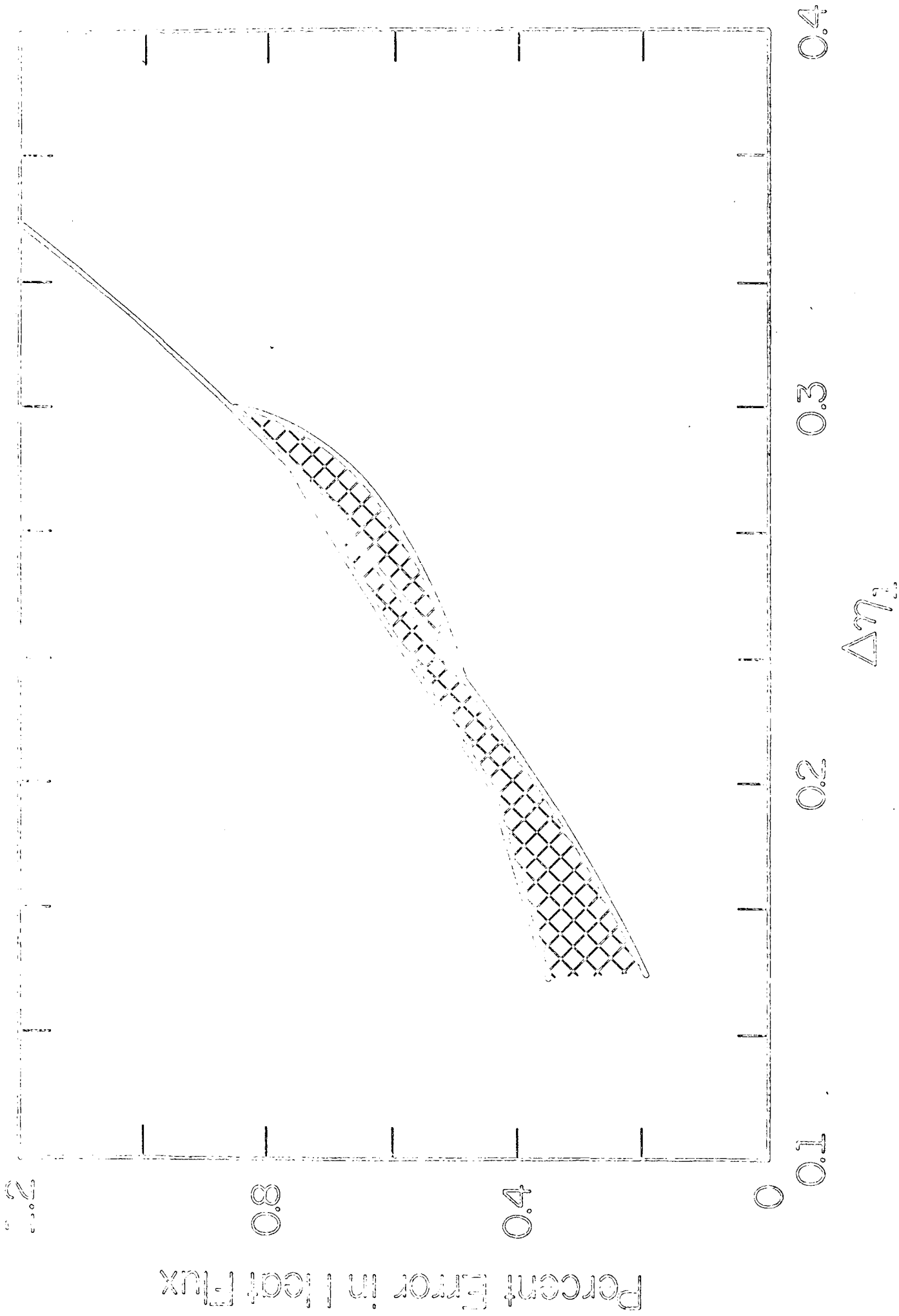


Figure 2.5 The Influence of Increment Changes on Accuracy, $\Delta\eta_c = 0.15$ (Semi-Infinite Solid with Step Change in Surface Temperature)

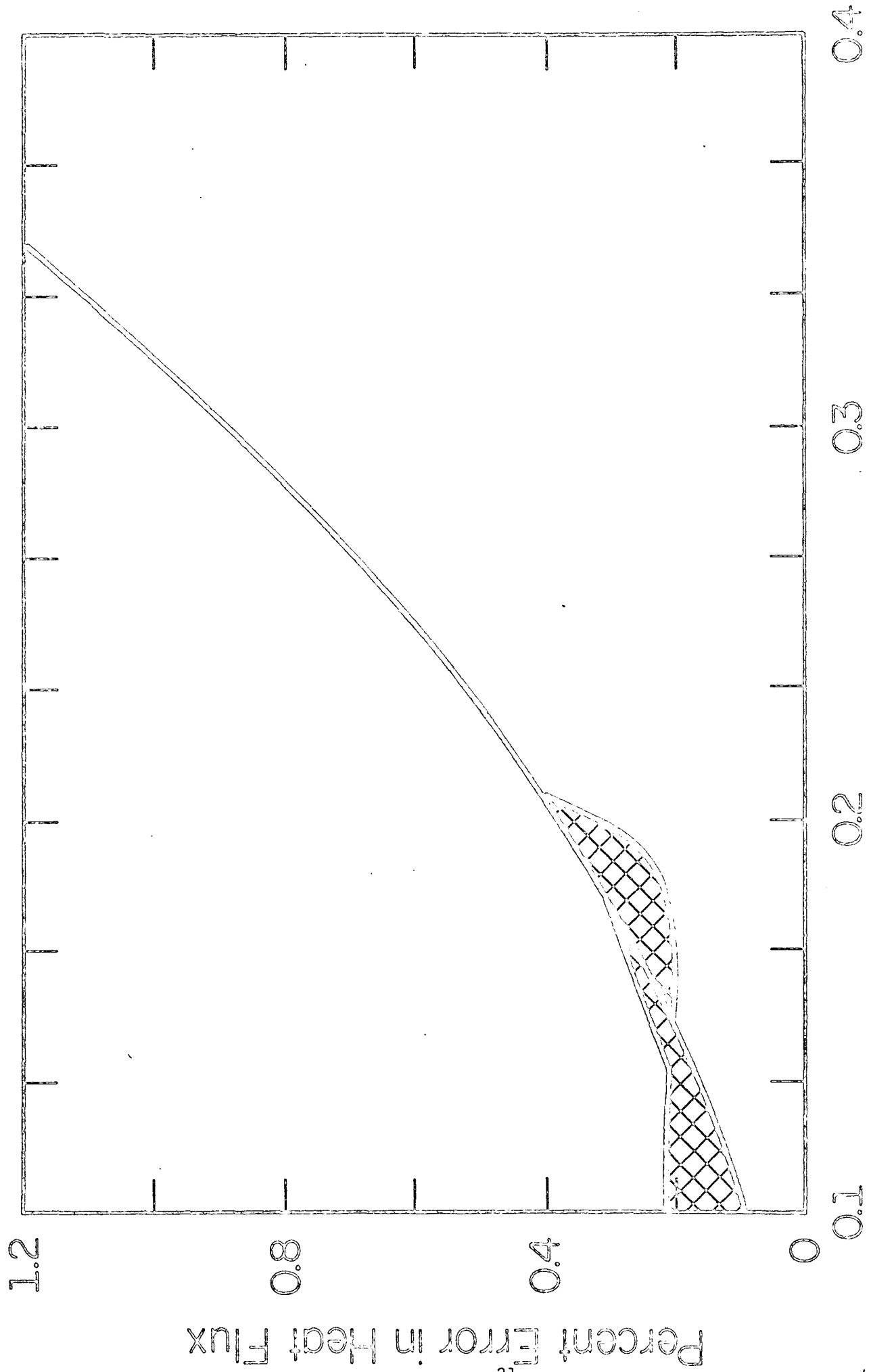


Figure 2.6 The Influence of Increment Changes on Accuracy, $\Delta\eta_c = 0.10$ (Semi-Infinite Solid with Step Change in Surface Temperature)

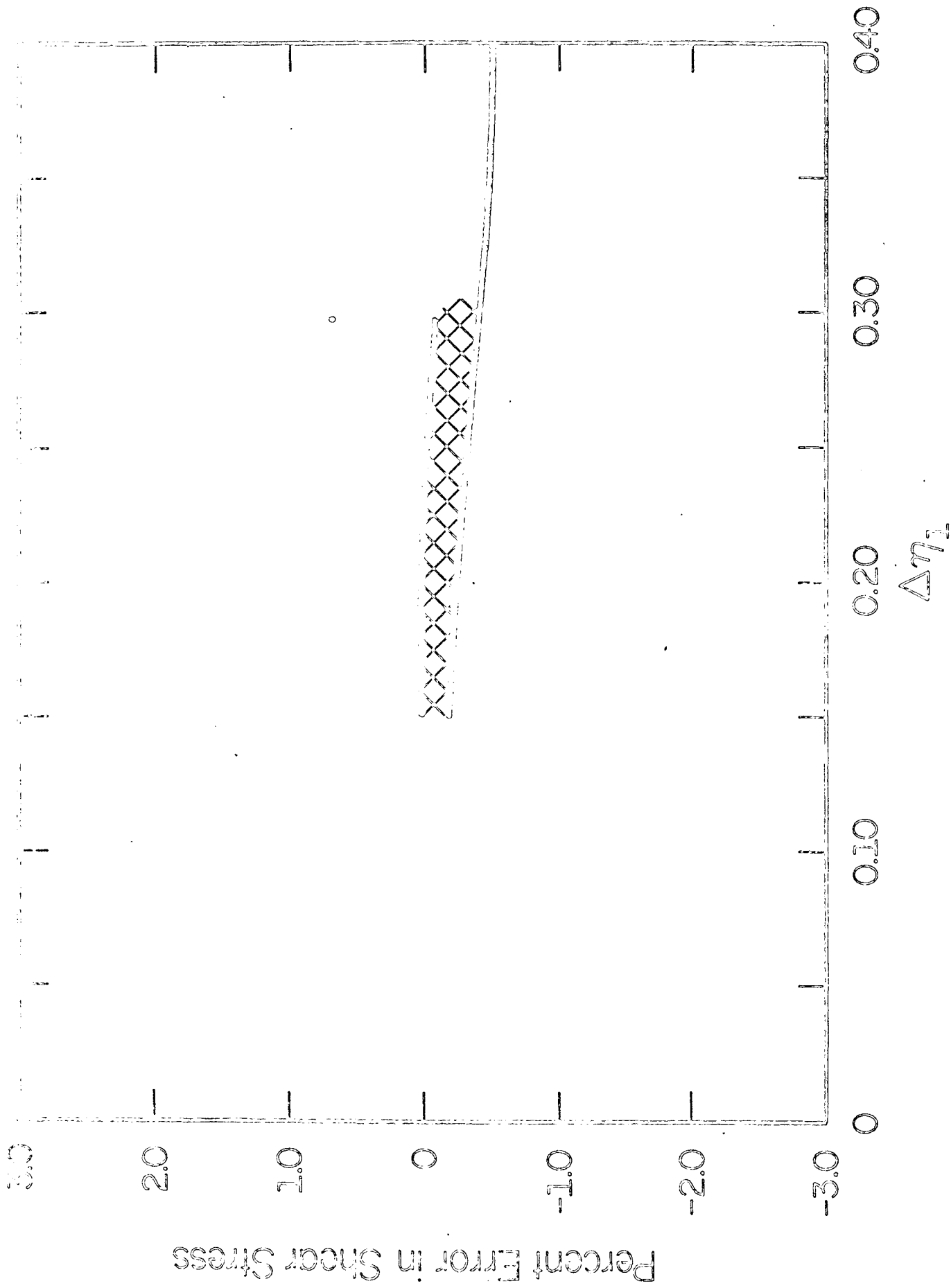


Figure 2.7 The Influence of Increment Change on Accuracy, $\Delta\eta_c = 0.15$ (The Blasius Problem)

3. FINITE DIFFERENCE ALGORITHMS WITH REPRESENTATIVE RESULTS

3.1 Algorithms for Compressible Flows of the Boundary Layer Type

As a result of the comprehensive study of the application of finite difference methods, three different algorithms were developed and employed in numerical experiments. These algorithms were presented in detail in an earlier report [1]. Many solutions of laminar incompressible flows were also given in [1], and pertinent results in graphical and tabular forms were presented in order to establish the accuracy of the algorithms. The advantages and disadvantages of each algorithm were discussed and, based on these considerations, the Crank-Nicolson algorithm was selected to solve the film cooling problem. Although the accuracy of the Crank-Nicolson method for compressible flows was demonstrated in a status report, the difference equations and the associated solution procedures were not presented. Hence, they will be given in this section.

The Crank-Nicolson method was employed to solve the film cooling problem for two reasons: First, this implicit method eliminates the problem of instability associated with explicit methods. Although the scheme results in simultaneous nonlinear equations, their solution does not generally require more computational effort per step than the explicit method. Second, the average differences generally result in greater accuracy compared to the Standard Implicit and Explicit methods. Some representative results showing the accuracy of the Crank-Nicolson algorithm for the solution of laminar incompressible and compressible boundary layer flows are given in Figs. 4 and 5 of [3].

The solution procedure associated with the Crank-Nicolson method will be described by an example. Consider the case of compressible boundary layer flow over a flat plate. Dimensionless variables are introduced in order to leave u_∞ , T_∞ , ρ_∞ , μ_∞ , and k_∞ unspecified. Specifically,

$$\rho^* = \frac{\rho}{\rho_\infty}, \quad u^* = \frac{u}{u_\infty}, \quad T^* = \frac{T}{T_\infty}, \quad \mu^* = \frac{\mu}{\mu_\infty}, \quad \text{and} \quad k^* = \frac{k}{k_\infty}$$

The governing difference equations derived from a physical model (see [1]) in terms of the dimensionless variables are:

Continuity:

$$(\rho^* v'^{\dagger})_{i, n+\frac{1}{2}} = (\rho^* v'^{\dagger})_{i-1, n+\frac{1}{2}} + \frac{1}{2} \left[(\rho^* u^*)_{i-1, n} + (\rho^* u^*)_{i, n} - (\rho^* u^*)_{i-1, n+1} - (\rho^* u^*)_{i, n+1} \right] \quad (45)$$

Momentum:

$$\begin{aligned} & (\rho^* u^*)_{i, n+\frac{1}{2}} (u_{i, n+1}^* - u_{i, n}^*) \\ & + (\rho^* v'^{\dagger})_{i, n+\frac{1}{2}} \left(\frac{u_{i+1, n+1}^* - u_{i-1, n+1}^* + u_{i+1, n}^* - u_{i-1, n}^*}{4} \right) \\ & = \frac{1}{2M} \left[\mu_{i+\frac{1}{2}, n+1}^* (u_{i+1, n+1}^* - u_{i, n+1}^*) + \mu_{i-\frac{1}{2}, n+1}^* (u_{i-1, n+1}^* - u_{i, n+1}^*) \right. \\ & \left. + \mu_{i+\frac{1}{2}, n}^* (u_{i+1, n}^* - u_{i, n}^*) + \mu_{i-\frac{1}{2}, n}^* (u_{i-1, n}^* - u_{i, n}^*) \right] \quad (46) \end{aligned}$$

Energy:

$$\begin{aligned} & (\rho^* u^*)_{i, n+\frac{1}{2}} (T_{i, n+1}^* - T_{i, n}^*) + (\rho^* v'^{\dagger})_{i, n+\frac{1}{2}} \left(\frac{T_{i+1, n+1}^* - T_{i-1, n+1}^* + T_{i+1, n}^* - T_{i-1, n}^*}{4} \right) \\ & = \frac{1}{2(\text{Pr})(M)} \left[k_{i+\frac{1}{2}, n+1}^* (T_{i+1, n+1}^* - T_{i, n+1}^*) \right. \\ & + k_{i-\frac{1}{2}, n+1}^* (T_{i-1, n+1}^* - T_{i, n+1}^*) + k_{i+\frac{1}{2}, n}^* (T_{i+1, n}^* - T_{i, n}^*) \\ & \left. + k_{i-\frac{1}{2}, n}^* (T_{i-1, n}^* - T_{i, n}^*) \right] \\ & \quad - \frac{(\gamma - 1) \text{Ma}^2}{16(M)} \mu_{i, n+\frac{1}{2}}^* (u_{i+1, n+1}^* - u_{i-1, n+1}^* + u_{i+1, n}^* - u_{i-1, n}^*)^2 \quad (47) \end{aligned}$$

Equation of State:

$$\rho^* T^* = 1 \quad (48)$$

Property Relationship:

$$\mu^* = k^* = (T^*)^\omega \quad (49)$$

where Pr and Ma are the Prandtl and Mach numbers, respectively. The quantities $(v')^{\dagger} = (v/u_{\infty}) (\Delta x/\Delta y)$, and $M \equiv [(\Delta y)^2 u_{\infty}]/(v_{\infty} \Delta x)$ were introduced in order that the spatial increments Δx and Δy could remain unspecified. The indices i, n represent the location $y_i = (i - 1)\Delta y$ and $x_n = n(\Delta x)$. Since u

and T are defined only at the discrete locations y_i and x_n , the quantities which must be known at the locations $y_{i+1/2}$ or $x_{n+1/2}$ are calculated as follows:

$$(\rho^*u^*)_{i, n+1/2} = \frac{1}{2} [(\rho^*u^*)_{i, n+1} + (\rho^*u^*)_{i, n}]$$

$$\mu_{i+1/2, n}^* = k_{i+1/2, n}^* = \left(\frac{T_{i+1, n}^* + T_{i, n}^*}{2} \right)^\omega$$

$$\mu_{i, n+1/2}^* = \left(\frac{T_{i, n+1}^* + T_{i, n}^*}{2} \right)^\omega$$

The initial and boundary conditions are

$$u_{i, 0}^* = 1 \quad \text{and} \quad T_{i, 0}^* = 1, \quad i > 0$$

$$u_{0, n}^* = v_{0, n}^{\dagger} = 0 \quad \text{and} \quad T_{0, n}^* = 1, \quad n \geq 0$$

$$u_{i, n}^* = 1 \quad \text{and} \quad T_{i, n}^* = 1, \quad n > 0, \quad i = I \quad (\text{where } I \text{ is large})$$

An examination of Eqs. (46) and (47) shows that if the quantities $(\rho^*u^*)_{i, n+1/2}$, $(\rho^*v^{\dagger})_{i, n+1/2}$, $\mu_{i+1/2, n+1}^*$, and $k_{i+1/2, n+1}^*$ were known, the equations would be linear. If these "unknown" quantities were approximated, Eqs. (46) and (47) could be solved iteratively, and the results from the iteration could be employed to correct these "unknowns" after each iteration. Numerical experiments indicated that the iteration process converges rapidly if the initial approximation to these "unknowns" is accurate.

A predictor for $u_{i, n+1}^*$ and $T_{i, n+1}^*$ was derived in [1] and is given by

$$\phi_{i, n+1}^{\circ} = 3\phi_{i, n} - 3\phi_{i, n-1} + \phi_{i, n-2}, \quad n > 1 \quad (50a)$$

where ϕ denotes either u^* or T^* . The expression is valid only for $n > 1$ and approximations for u^* and T^* are also required for n equal to zero and one. A linear extrapolation is used for $n = 1$; that is

$$\phi_{i, 2}^{\circ} = 2\phi_{i, 1} - \phi_{i, 0} \quad (50b)$$

and the initial condition is used for $n = 0$; that is

$$\phi_{i, 1}^{\circ} = \phi_{i, 0} \quad (50c)$$

The approximation for $\phi_{i,1}^{\circ}$ is arbitrary so long as the iteration converges. Equation (50a) is identical to that which is obtained by equating the second central differences

$$\delta_x^2 \phi_{i,n} = \delta_x^2 \phi_{i,n-1}$$

Thus, if $\delta_x^2 \phi_{i,n}$ and $\delta_x^2 \phi_{i,n-1}$ are of opposite sign, Eq. (50a) would give an inaccurate prediction for $\phi_{i,n+1}^{\circ}$. This difficulty had been encountered in some laminar and turbulent problems. Several other predictors were tested and two were found which avoided this difficulty and also gave accurate predictions. One of them is the Standard Explicit method (see [1]) but its application is limited to incompressible problems. The other one is

$$\delta_x^2 \phi_{i,n} = \delta_x^2 \phi_{i,n-2}$$

or

$$\phi_{i,n+1}^{\circ} = \phi_{i,n} + \delta_x \phi_{i,n-1/2} + \delta_x \phi_{i,n-3/2} - \delta_x \phi_{i,n-5/2}, \quad n > 2 \quad (51)$$

For $n \leq 2$, $\delta_x \phi_{i,-1/2}$, $\delta_x \phi_{i,-3/2}$ and $\delta_x \phi_{i,-5/2}$ were assumed to be zero. These assumptions are arbitrary as long as the solution converges. Equation (51) does not require additional computational effort compared to Eq. (50a) if the central differences are stored.

A method of solution which is similar to the predictor-corrector methods employed in the solution of ordinary differential equations is used. A "predictor", Eqs. (50) or (51), is employed to predict $u_{i,n+1}^*$ and $T_{i,n+1}^*$. Next, the continuity equation, the equation of state, and the property relationships are used to obtain $(\rho^* v^{\dagger})_{i,n+1/2}$, ρ^* , μ^* , and k^* . Then the momentum and energy equations, the "correctors", are used iteratively to correct the discrete velocities and temperatures, and to add the required stability to the overall process. The continuity equation is employed after each application of either "corrector" to correct $(\rho^* v^{\dagger})_{i,n+1/2}$. μ , ρ , and k are recalculated only after each application of the energy equation. Since the predictor provides accurate estimates of the required dependent variables after the first few steps, the correctors usually must be applied only once.

After the quantities $\rho^* u^*$, $\rho^* v^{\dagger}$, μ^* , and k^* are calculated, Eqs. (46)

and (47) can be rewritten in the form

$$A_i \phi_{i-1, n+1}^K + B_i \phi_{i, n+1}^K + C_i \phi_{i+1, n+1}^K = b_i, \quad 1 < i \leq I \quad (52)$$

where A_i , B_i , C_i , and b_i are all known quantities. The superscript K denotes the k th approximation obtained from the corrector; $K = 0$ corresponds to the prediction. Thus, the momentum and the energy equations are reduced to two sets of linear algebraic equations with tridiagonal coefficient matrices. The simultaneous equations are solved by employing the algorithm of Section 3.1 of [6].

Since the corrector must be applied iteratively, a means of terminating this iterative process is required. A test obtained from the conservation of mass is

$$(100 \text{ percent}) \left| \frac{\left[(\rho^* v'^{\dagger})_{I, n+1/2} \right]^K - \left[(\rho^* v'^{\dagger})_{I, n+1/2} \right]^{K-1}}{\left[(\rho^* v'^{\dagger})_{I, n+1/2} \right]^K} \right| \leq \epsilon \quad (53a)$$

The expression in the left-hand side of Eq. (53a) is equal to $1/\Delta y$ times the change between iterations of mass flow out of the control volume across the surface perpendicular to the plate at location $n + 1$. To reduce the probability of accidentally satisfying Criterion (53a), a second criterion

$$(100 \text{ percent}) \left| \frac{\left[(\rho^* u^*)_{2, n+1} \right]^K - \left[(\rho^* u^*)_{2, n+1} \right]^{K-1}}{\left[(\rho^* u^*)_{2, n+1} \right]^K} \right| \leq 0.1 \epsilon \quad (53b)$$

is introduced. Criterion (53b) is generally less stringent than Criterion (53a). Numerical results showed that $\epsilon = 1$ is sufficiently stringent for engineering calculations.

Finally, some of the advantages of the algorithms being developed in this study in contrast to many of those described in the literature are:

1. The solution is effected in the physical plane. This makes the algorithms more general and enables their adaptation to a variety of problems with little or no modification. The physical variables are available for direct examination; hence, the characteristics of the problem are more easily discovered.

2. No initial condition is required in v or $\partial u/\partial x$. Many techniques reported in the literature require such conditions. These conditions are incompatible with the boundary layer approximations.
3. The finite difference equations are based on a physical model; hence, the derivation of expressions for the wall shear stress, the wall heat flux, and the boundary conditions can be accomplished in a rational manner which is consistent with the approximations employed in the interior of the flow field.

3.2 A Turbulent Model and the Associated Finite Difference Procedure

Consider the case of two-dimensional, incompressible, turbulent flow, the governing mean flow equations employing an eddy viscosity concept are (see [4]):

$$\frac{\partial \bar{u}}{\partial x} + \frac{\partial \bar{v}}{\partial y} = 0 \quad (54)$$

$$\rho \left(\bar{u} \frac{\partial \bar{u}}{\partial x} + \bar{v} \frac{\partial \bar{u}}{\partial y} \right) = - \frac{d\bar{p}}{dx} + \frac{\partial}{\partial y} \left[(\mu + A_\tau) \frac{\partial \bar{u}}{\partial y} \right] \quad (55)$$

where \bar{u} , \bar{v} are the mean velocities, $u = \bar{u} + u'$, \bar{p} is the mean pressure, and A_τ is the turbulent mixing coefficient which is often called the "eddy" viscosity. A_τ is defined as

$$A_\tau = \frac{-\overline{\rho u' v'}}{d\bar{u}/dy}$$

where u' , v' are the velocities of fluctuations. Equations (54) and (55) are made to correspond to the incompressible, laminar boundary layer equations by introducing an effective viscosity

$$\mu_e = \mu + A_\tau \quad (56)$$

Hence, the finite difference algorithms of [1] can be employed to effect a solution. A_τ is not a property of the fluid like μ , but is dependent upon the mean velocity \bar{u} . In this preliminary investigation, Prandtl's mixing length hypothesis was employed in the viscosity model, thus, Eq. (56) becomes

$$\mu_e = \mu + \rho \ell^2 \left| \frac{\partial \bar{u}}{\partial y} \right| \quad (57)$$

where ℓ is the mixing length. The mixing length expressions employed are given by:

$$\frac{\ell}{\delta} = 0.41 [1 - \exp(-y^+/26)] (y/\delta), \quad y/\delta \leq 0.1 \quad (58a)$$

$$\frac{\ell}{\delta} = [0.41 (y/\delta) - 1.53506 \zeta^2 + 2.75625 \zeta^3 - 1.88425 \zeta^4] [1 - \exp(-y^+/26)], \quad 0.1 \leq y/\delta \leq 0.6 \quad (58b)$$

$$\frac{\ell}{\delta} = 0.089, \quad y/\delta > 0.6 \quad (58c)$$

where

$$y^+ = \frac{\rho}{\mu} \left(\frac{\tau_w}{\rho} \right)^{1/2} y$$

$$\zeta = (y/\delta - 0.1)$$

and δ is the boundary layer thickness. Equation (58) is a modification of Pletcher's expressions [7]. Pletcher's expressions were modified in order to avoid the discontinuity in ℓ/δ at $y/\delta = 0.1$ which occurs if y^+ is small.

If the turbulent boundary layer equations were to be solved by a finite difference technique employing a uniform network, small increments are required in order to include grid points in the laminar sub-layer. However, the thickness of this layer is small relative to the thickness of the boundary layer; *e.g.*, for $Re_x = 1.87 \times 10^7$, $y_\delta^+ = 12,000$ [4], if an increment of $\Delta y^+ = 4$ is employed, it would require 3,000 grid points in the normal direction. Hence, a nonuniform network must be used. This consideration provided the impetus for the study presented in Section 2.3.

The finite difference equations and the associated solution procedure for the case of turbulent flow over a flat plate will be considered. The nonuniform increments are given by the following geometrical progressions.

$$\Delta y_i = r_y^{i-1} \Delta y_1, \quad i \geq 1 \quad (22)$$

and

$$\Delta x_n = r_x^{n-1} \Delta x_1, \quad n \geq 1 \quad (59)$$

Therefore,

$$y_i = \Delta y_1 \left(\frac{r_y^{i-1} - 1}{r_y - 1} \right), \quad i \geq 1 \quad (24)$$

and

$$x_n = \Delta x_1 \left(\frac{r_x^n - 1}{r_x - 1} \right), \quad n \geq 0 \quad (60)$$

The governing difference equations obtained by employing the Crank-Nicolson method are:

Continuity:

$$(\bar{v}')_{i, n+1/2}^\dagger = \frac{(\bar{v}')_{i-1, n+1/2}^\dagger}{r_y} + \frac{1}{2} (\bar{u}_{i-1, n}^* + \bar{u}_{i, n}^* - \bar{u}_{i-1, n+1}^* - \bar{u}_{i, n+1}^*) \quad (61)$$

Momentum:

$$\begin{aligned} & \bar{u}_{i, n+1/2}^* (\bar{u}_{i, n+1}^* - \bar{u}_{i, n}^*) + \frac{(\bar{v}')_{i, n+1/2}^\dagger}{2r_y(1+r_y)} \left\{ \left[\bar{u}_{i+1, n+1}^* + (r_y^2 - 1) \bar{u}_{i, n+1}^* - r_y^2 \bar{u}_{i-1, n+1}^* \right] \right. \\ & \left. + \left[\bar{u}_{i+1, n}^* + (r_y^2 - 1) \bar{u}_{i, n}^* - r_y^2 \bar{u}_{i-1, n}^* \right] \right\} = \left[\frac{r_x^n}{(1+r_y)(r_y^{i-2})^2 M_1} \right] \\ & \cdot \left\{ \left[\frac{\mu_{i+1/2, n+1}^*}{r_y} (\bar{u}_{i+1, n+1}^* - \bar{u}_{i, n+1}^*) + \mu_{i-1/2, n+1}^* (\bar{u}_{i-1, n+1}^* - \bar{u}_{i, n+1}^*) \right] \right. \\ & \left. + \left[\frac{\mu_{i+1/2, n}^*}{r_y} (\bar{u}_{i+1, n}^* - \bar{u}_{i, n}^*) + \mu_{i-1/2, n}^* (\bar{u}_{i-1, n}^* - \bar{u}_{i, n}^*) \right] \right\} \quad (62) \end{aligned}$$

where

$$\bar{u}^* = \frac{\bar{u}}{u_\infty}, \quad (\bar{v}')_{i, n+1/2}^\dagger = \frac{\bar{v}_{i, n+1/2}}{u_\infty} \left(\frac{\Delta x_{n+1}}{\Delta y_{i-1, n+1}} \right)$$

$$\mu^* = 1 + \frac{\rho u_\infty}{\mu} \ell^2 \left| \frac{\partial \bar{u}^*}{\partial y} \right|$$

and

$$M_1 \equiv \frac{u_\infty (\Delta y_1)^2}{\nu (\Delta x_1)} \quad (63)$$

Lastly, the expressions for μ^* and l/δ in difference form are:

$$\mu_{i+\frac{1}{2}, n+1}^* = 1 + (\text{Re}_1^\dagger M_1)^{\frac{1}{2}} \left(\frac{l}{\delta}\right)_{i+\frac{1}{2}, n+1}^2 (i_\delta - 1)^2 \frac{|\bar{u}_{i+1, n+1}^* - \bar{u}_{i, n}^*|}{r_y^{i-1}} \quad (64)$$

$$\left(\frac{l}{\delta}\right)_{i+\frac{1}{2}, n+1} = 0.41 [1 - \exp(-y_{i+\frac{1}{2}, n+1}^+ / 26)] \left(\frac{y}{\delta}\right)_{i+\frac{1}{2}, n+1},$$

$$\left(\frac{y}{\delta}\right)_{i+\frac{1}{2}, n+1} \leq 0.1 \quad (65a)$$

$$\left(\frac{l}{\delta}\right)_{i+\frac{1}{2}, n+1} = \left[0.41 \left(\frac{y}{\delta}\right)_{i+\frac{1}{2}, n+1} - 1.53506 \zeta_{i+\frac{1}{2}, n+1}^2 + 2.75625 \zeta_{i+\frac{1}{2}, n+1}^3 - 1.88425 \zeta_{i+\frac{1}{2}, n+1}^4 \right] \left[1 - \exp(-y_{i+\frac{1}{2}, n+1}^+ / 26) \right],$$

$$0.1 \leq (y/\delta)_{i+\frac{1}{2}, n+1} \leq 0.6 \quad (65b)$$

$$\left(\frac{l}{\delta}\right)_{i+\frac{1}{2}, n+1} = 0.089, \quad \frac{y}{\delta}_{i+\frac{1}{2}, n+1} > 0.6 \quad (65c)$$

where

$$\text{Re}_1^\dagger = \frac{u_\infty (\Delta x_1)}{\nu} \quad (66)$$

$$y_{i+\frac{1}{2}, n+1}^+ = (\text{Re}_1^\dagger M_1)^{\frac{1}{4}} (\tilde{\Delta}_y \bar{u}_{i, n+1}^*)^{\frac{1}{2}} \left(i_e - 1 + \frac{r_y^{i-1}}{2} \right)$$

$$\left(\frac{y}{\delta}\right)_{i+\frac{1}{2}, n+1} = \frac{[i_e - 1 + (r_y^{i-1} / 2)]}{(i_\delta - 1)}$$

$$\zeta_{i+\frac{1}{2}, n+1} = \left[\left(\frac{y}{\delta}\right)_{i+\frac{1}{2}, n+1} - 0.1 \right]$$

$$i_e = 1 + \left(\frac{r_y^{i-1} - 1}{r_y - 1} \right) \quad (26)$$

i_δ is the location corresponding to the edge of the boundary layer, it is usually found by interpolation because the velocities are known only at discrete locations. $\tilde{\Delta}_y$ is the operator employed in calculating the

derivatives at the wall; it is given by*

$$\tilde{\Delta}_y \phi_1 = \frac{C_4 \phi_4 + C_3 \phi_3 + C_2 \phi_2 + C_1 \phi_1}{C_5} \quad (67)$$

where

$$C_1 = -r_y^3 (r_y + 2)(2r_y^2 + 4r_y + 3)$$

$$C_2 = 2r_y^6 + 8r_y^5 + 13r_y^4 + 11r_y^3 + 5r_y^2 + 2r_y$$

$$C_3 = -(2r_y^4 + 5r_y^3 + 5r_y^2 + 3r_y + 2)$$

$$C_4 = r_y + 2$$

$$C_5 = 2r_y^3 (r_y + 1)^3$$

The initial and boundary conditions are the same as that of the Blasius problem and are not repeated.

An examination of the difference equations show that neither Δx nor Δy needs to be specified to effect the solution; M_1 , Re_1^\dagger , r_x , r_y , I , and N (or their equivalent values, Eqs. (26) and (27)) are the only parameters needed. The solution procedure employed is the same as that described in [1] with the following exceptions:

1. The "predictor" used is Eq. (51) instead of Eq. (50). Although Eq. (51) was derived for uniform x-increment, it provided accurate predictions for $u_{i, n+1}$ for the nonuniform x-increment cases as expected.
2. The effective viscosity must be recalculated after the application of the "corrector", because the eddy viscosity is a function of \bar{u} .

Figure 3.1 shows the influence of Re_1^\dagger , r_x , and r_y on the accuracy of the local skin friction coefficient, c_f' . The results are preliminary; further investigation of the influence of M_1 and increment changes is planned.

*See [1] for the derivation of this operator for $r_y = 1$.

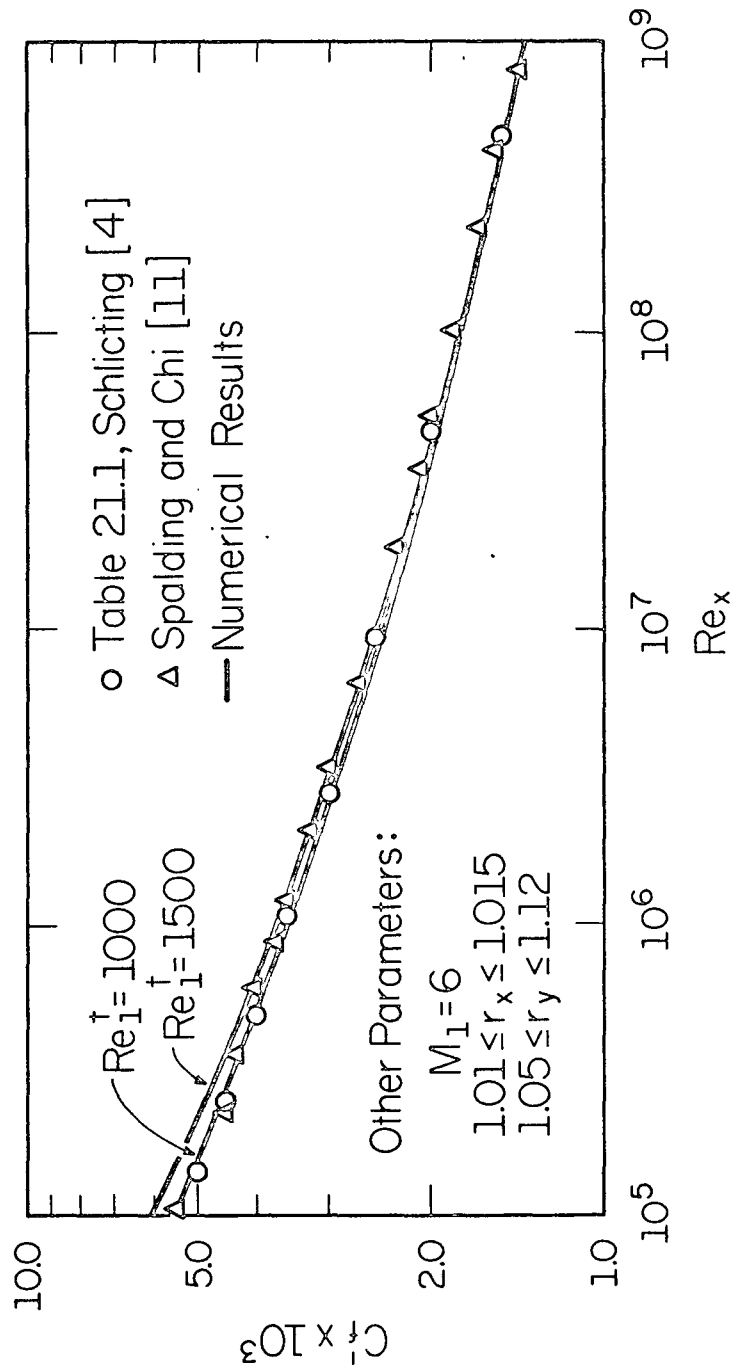


Figure 3.1 The Influence of r_x , r_y and Re_1^+ on the Accuracy of c_f^{+-} in Incompressible Turbulent Boundary Layer Flow

4. RESULTS FROM THE STUDY OF FILM COOLING

Results for laminar incompressible film cooling neglecting viscous dissipation were presented in [1]. Results obtained with a simplified model for laminar gaseous film cooling including the influences of compressibility and viscous dissipation will be presented here. These results are presented in generalized form, where the generalized independent variables were obtained by the techniques given in [3].

Gaseous film cooling involves the mixing of two moving streams in the vicinity of a solid wall. A coolant or secondary stream with a velocity u_s and a temperature T_s is ejected through a slot in a direction tangent to the surface. The objective is to protect the surface from the high temperature external stream, the primary stream, whose velocity and temperature are u_p and T_p . The primary flow in the case of interest is a supersonic and semi-infinite stream. It is assumed that a converging nozzle is employed for the coolant flow; hence, the velocity at the exit of the slot is either sonic or subsonic.

Figure 4.1 shows the flow configuration studied. This flow configuration results when the pressure of the secondary stream at the slot exit is equal to the pressure of the primary stream. The splitter plate is assumed to have zero thickness; hence, no expansion fans or shock waves will be present. The following assumptions were employed:

1. The flow field is laminar, two-dimensional and steady.
2. The secondary and primary fluids are the same and are ideal fluids. All relevant fluid properties are functions of temperature only.
3. At the exit of the slot, the secondary flow is either subsonic or sonic and the primary flow is supersonic. The static pressure of the secondary flow at this location is equal to the static pressure of the primary flow; hence, the flow configuration of Fig. 4.1 is obtained.
4. The boundary layer equations are valid in both regions I and II. (These regions are defined in Fig. 4.1.)

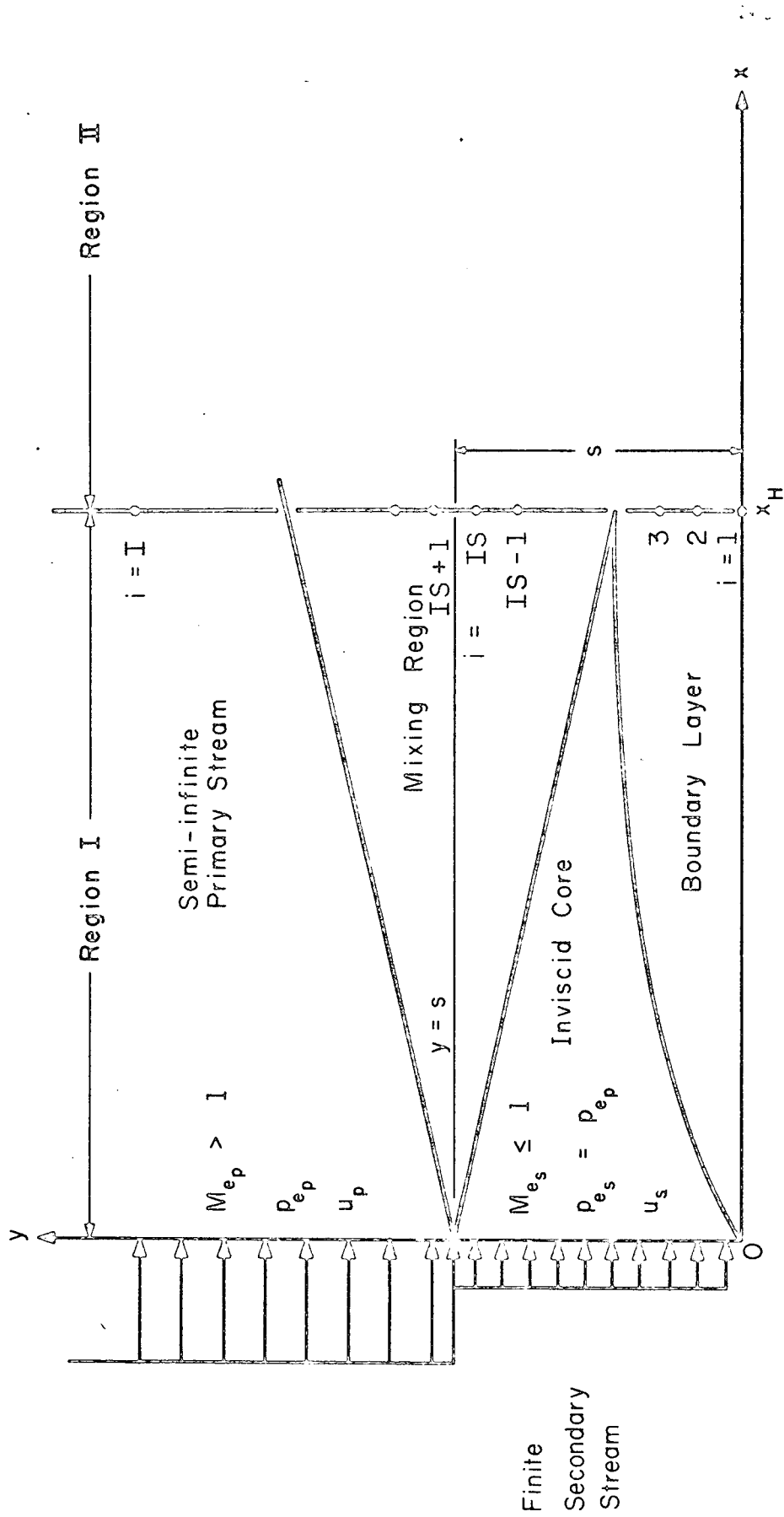


Figure 4.1 Nomenclature and Coordinate System for Flow Configuration being Studied

5. The free stream pressure and temperature do not vary in a direction along the film cooled surface.
6. The initial velocity and temperature profiles of both streams are uniform and the velocity vectors are parallel.
7. The splitter plate which initially separates the two streams has zero thickness at $x = 0$.
8. Heat transfer by thermal radiation is negligible.
9. The surface is isothermal and at the temperature of the secondary stream, T_s .

The governing equations with these assumptions are:

Continuity:

$$\frac{\partial}{\partial x} (\rho u) + \frac{\partial}{\partial y} (\rho v) = 0 \quad (68)$$

Momentum:

$$\rho \left(u \frac{\partial u}{\partial x} + v \frac{\partial u}{\partial y} \right) = \frac{\partial}{\partial y} \left(\mu \frac{\partial u}{\partial y} \right) \quad (69)$$

Energy:

$$\rho c_p \left(u \frac{\partial T}{\partial x} + v \frac{\partial T}{\partial y} \right) = \frac{\partial}{\partial y} \left(k \frac{\partial T}{\partial y} \right) + \mu \left(\frac{\partial u}{\partial y} \right)^2 \quad (70)$$

Equation of State:

$$\rho T = \frac{P}{R} = \text{a constant} \quad (71)$$

Property Relations:

$$\mu = \mu(T), \quad k = k(T), \quad \text{and} \quad c_p = c_p(T) \quad (72)$$

The initial boundary conditions are

$$\text{at } x = 0, \quad u = u_s \quad \text{and} \quad T = T_s, \quad y \leq s$$

$$u = u_p \quad \text{and} \quad T = T_p, \quad y > s$$

$$\text{at } y = 0 \quad u = v = 0 \quad \text{and} \quad T = T_s$$

$$x > 0$$

$$\text{at } y \rightarrow \infty \quad u = u_\infty = u_p \quad \text{and} \quad T = T_\infty = T_p$$

The property relations remain to be specified. It will be assumed that the Prandtl number and the specific heat are constants. Thus, μ is proportional to k and a single function needs to be specified. The viscosity can be accurately specified by Sutherland's formula

$$\frac{\mu}{\mu_0} = \left(\frac{T}{T_0} \right)^{3/2} \frac{T_0 + S_1}{T + S_1} \quad (73)$$

where μ_0 is the viscosity at the reference temperature T_0 which can be chosen arbitrarily and S_1 is Sutherland's constant. On the other hand, a simple power law

$$\frac{\mu}{\mu_0} = \left(\frac{T}{T_0} \right)^\omega \quad (74)$$

is often used because this less accurate law gives rise to one less parameter if T/T_0 is employed as the dimensionless temperature. For this reason it was used in this investigation. A more accurate expression, such as Sutherland's formula, as well as variable specific heat could be easily incorporated into the finite difference algorithm.

Figures 4.2 through 4.5 show the results of compressible film cooling. In order to illustrate vividly the effectiveness of cooling, the shear stress, the heat flux at the wall, and the total rate of heat transfer are normalized by the corresponding values for zero slot height. Specifically,

$$\tilde{\tau} \equiv \frac{\tau_w}{\tau_w|_{s=0}}, \quad \tilde{q}_w'' = \frac{q_w''}{q_w''|_{s=0}}, \quad \tilde{q} = \frac{q}{q|_{s=0}}$$

The results in these figures were obtained with $\omega = 1$, $\gamma = 1.4$, and $Pr = 1$. These values were chosen only because $\tau|_{s=0}$, $q''|_{s=0}$, and $q|_{s=0}$ are known for this case and do not have to be obtained numerically.

Figure 4.2 shows a family of temperature profiles. The parameter is the dimensionless x-location, $\xi = (x/s)(v_\infty/u_\infty)$. The change in the heating rate can be clearly seen by examining the slopes at y/s equal to zero. Figure 4.3 shows the variation of the normalized heat flux at the wall with the dimensionless x-location, ξ . The velocity ratio,

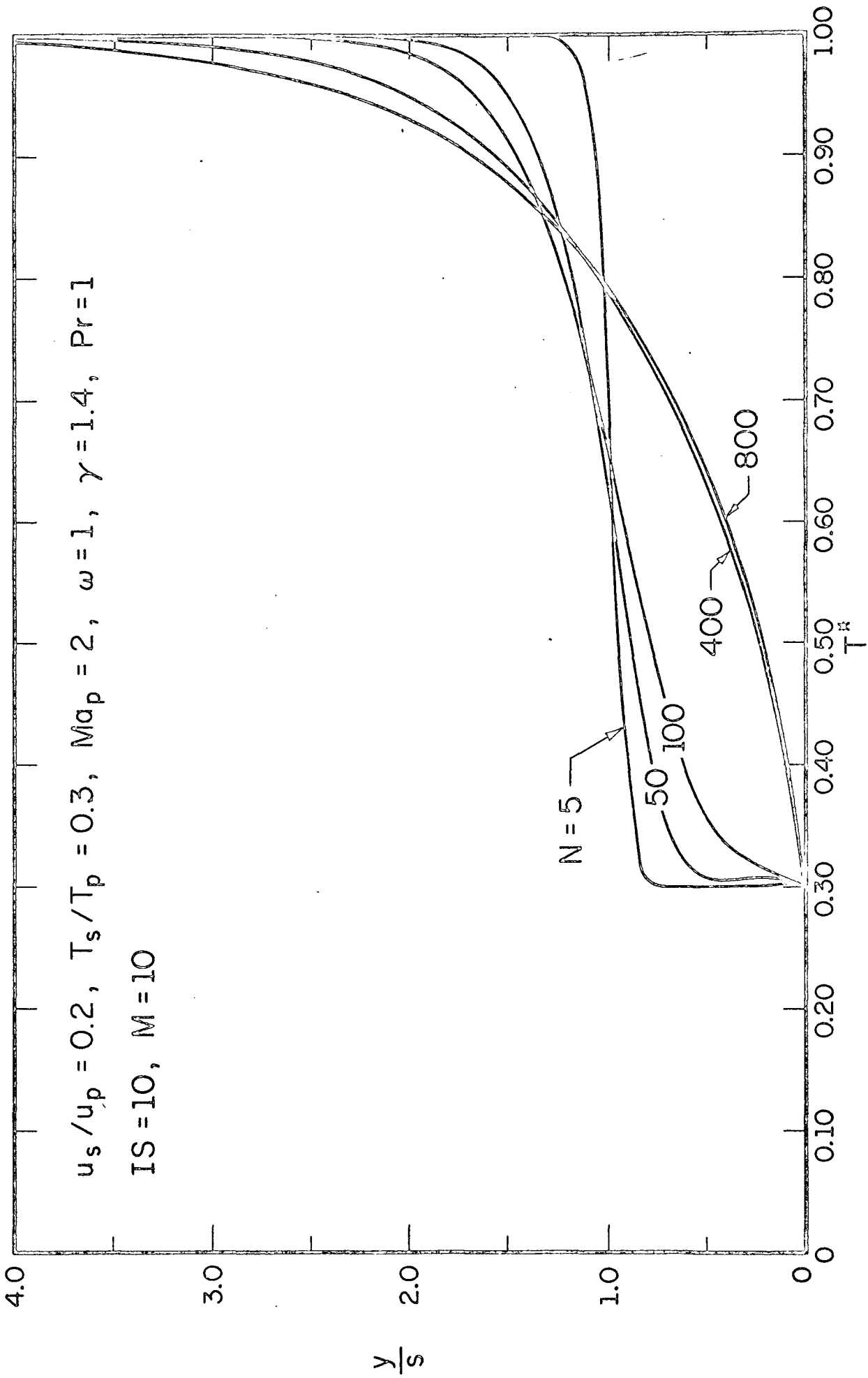


Figure 4.2 The Variation of the Temperature Distribution with N or $\xi - \xi = 0.001107 N$

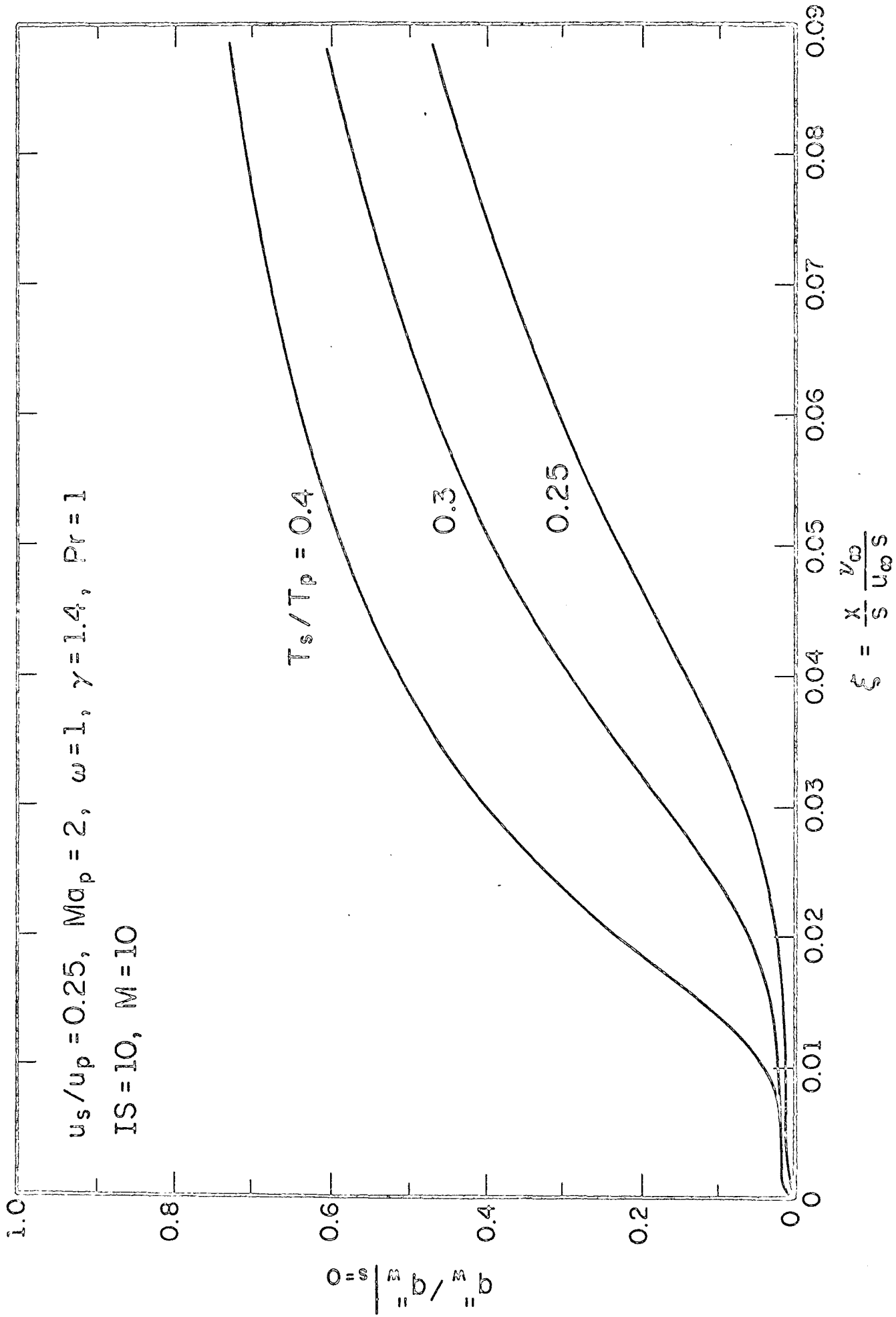


Figure 4.3 The Influence of T_s/T_p on the Normalized Heat Flux

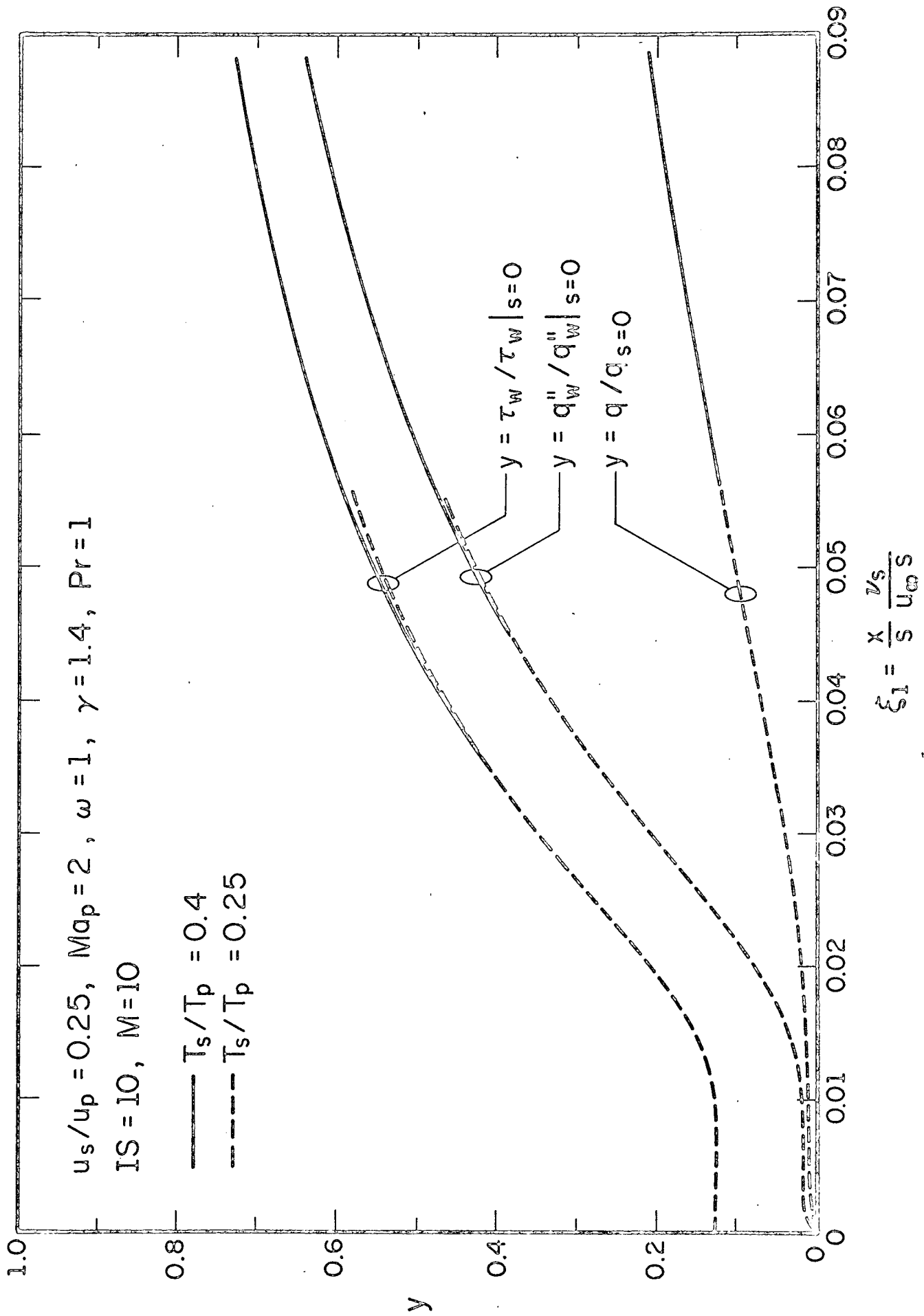


Figure 4.4 The Influence of T_s/T_p on the Normalized Wall Shear Stress, Heat Flux, and Total Heat Flow Rate

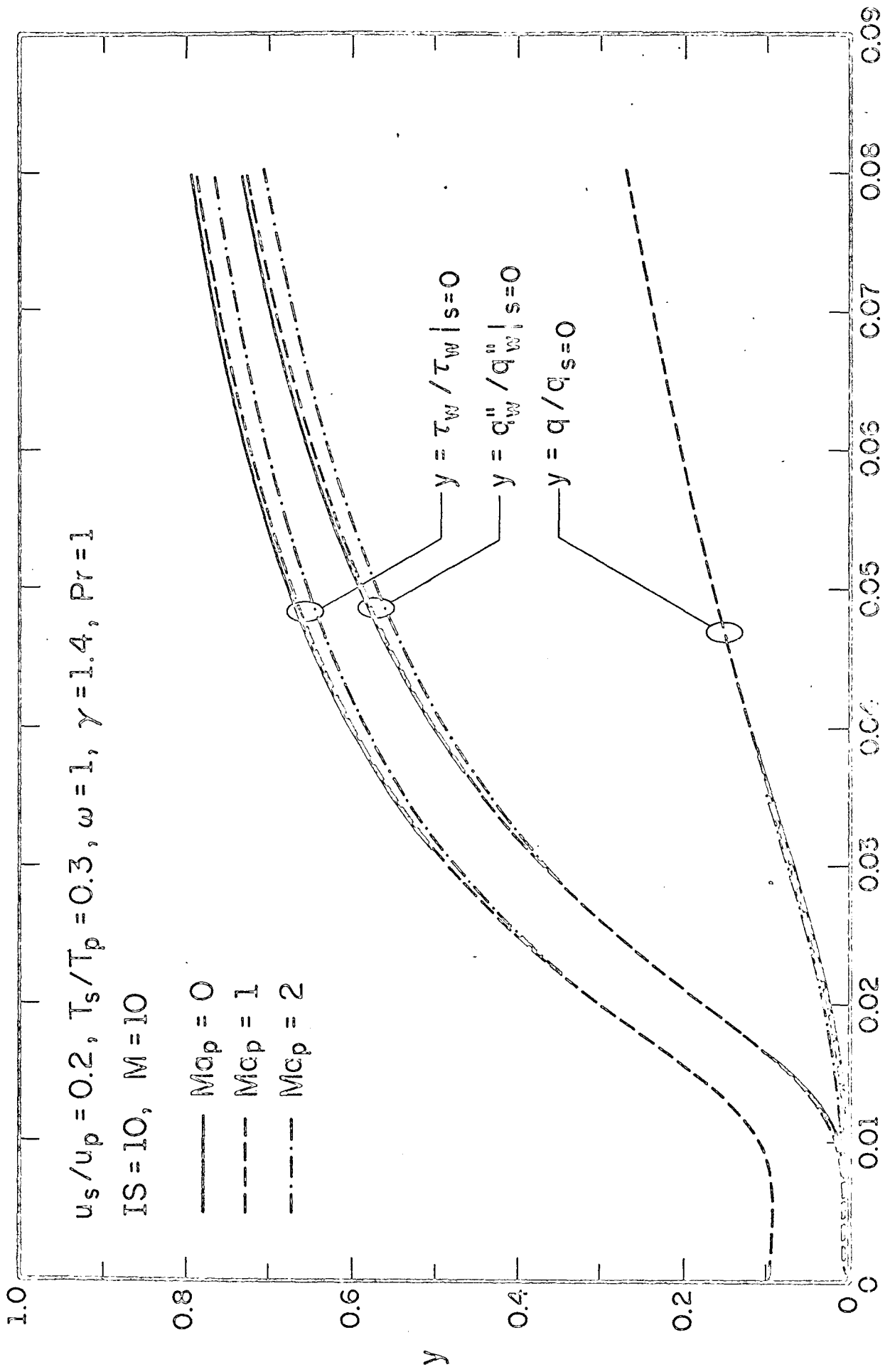


Figure 4.5 The Influence of Ma_p on the Normalized Wall Shear Stress, τ_w and Normalized Heat Flux, q''_w and Normalized Heat Flux, q at $F = 1$

u_s/u_p , is 0.25 and the Mach number of the primary stream, Ma_p , is equal to two; the parameter is the temperature ratio, T_s/T_p . Figure 4.4 shows the same results including, in this case, also the the normalized shear stress and heat flow rate with a new dimensionless x-coordinate, defined as $\xi_1 = (x/S)(v_s/u_\infty S) = (T_s/T_p)^{\omega+1} \xi$. The normalized shear stress, heat flux, and total heat flow rate become, for practical purposes, independent of T_s/T_p when ξ_1 is used for the abscissa in place of ξ .

Figure 4.5 shows the variation of the normalized wall shear stress, wall heat flux, and total heat flow rate with the dimensionless x-location, $\xi_1 = (x/S)(v_s/u_\infty S)$. The velocity ratio is 0.2 and the temperature ratio is 0.3; the parameter is the Mach number. The plots show the influence of Mach number on the heat flow ratio to be small.

In this analysis, the primary stream is assumed to be uniform which is unrealistic in most applications. Hence, the results are upper limits of the more practical case with an initial boundary layer in the primary stream. Furthermore, the assumptions of laminar flow is quite restrictive. The mixing region, in most practical cases, will be turbulent. The boundary layer which forms along the wall will be laminar initially but will become turbulent at a relatively low Reynolds number due to the turbulence in the neighboring mixing region. Hence, the turbulent case is now being investigated. The preliminary results of Sections 2.3 and 3.2 stemmed from this effort. Some of the other assumptions currently being used also need to be examined more closely.

PRECEDING PAGE BLANK NOT FILMED

5. REFERENCES

1. Clausing, A. M., "Finite Difference Solutions of the Boundary Layer Equations," Mechanical Engineering Technical Report 138-1, University of Illinois at Urbana-Champaign, Urbana, Ill., 1970.
2. Clausing, A. M., "Similarity and Generalized Finite-Difference Solutions of Parabolic Partial Differential Equations," J. of Applied Mechanics, Vol. 39, Trans. ASME, Vol. 94, Series E, 1972, pp. 584-590.
3. Clausing, A. M., "Practical Techniques for Estimating the Accuracy of Finite-Difference Solutions to Parabolic Equations," to be published in J. of Applied Mechanics, ASME Paper No. 72-WA/APM-12, 1972.
4. Schlichting, H., Boundary-Layer Theory, Sixth Edition, McGraw-Hill Book Co., New York, 1968.
5. Young, D., "The Numerical Solution of Elliptic and Parabolic Partial-Differential Equations," Survey of Numerical Analysis, Todd, J., editor, McGraw-Hill Book Co., New York, 1962.
6. Clausing, A. M., "Numerical Methods in Heat Transfer," Advanced Heat Transfer, Chao, B. T., editor, University of Illinois Press, Urbana, Ill., 1969, pp. 157-216.
7. Pletcher, R. N., "On a Finite-Difference Solution for the Constant-Property Turbulent Boundary Layer," AIAA Journal, Vol. 7, 1969, pp. 305-311.
8. Smith, A. M. O. and Cebeci, T., "Solution of the Boundary-Layer Equations for Incompressible Turbulent Flow," Proceedings of the 1968 Heat Transfer and Fluid Mechanics Institute, Stanford, Cal., 1968, pp. 174-191.
9. Harris, J. E., "Numerical Solution of the Equations for Compressible Laminar, Transitional and Turbulent Boundary Layers and Comparison with Experimental Data," NASA TR R-368, August 1971, p. 32.
10. Adams, J. C., "Eddy Viscosity-Intermitting Factor Approach to Numerical Calculation of Transitional Heating on Sharp Cones in Hypersonic Flow," AEDC-TR-70-210, Nov. 1970.
11. Spalding, D. B. and Chi, S. W., "The Drag of a Compressible Turbulent Boundary Layer on a Smooth Flat Plate With and Without Heat Transfer," J. of Fluid Mechanics, Vol. 18, Part 1 (Jan. 1964), pp. 117-143.

Preceding page blank